



# Evidence from the resurrected family *Polyrhabdinidae* Kamm, 1922 (Apicomplexa: Gregarinomorpha) supports the epimerite, an attachment organelle, as a major eugregarine innovation

Gita G. Paskerova<sup>1</sup>, Tatiana S. Miroljubova<sup>2</sup>, Andrea Valigurová<sup>3</sup>, Jan Janoušek<sup>4</sup>, Magdaléna Kováčiková<sup>3</sup>, Andrei Diakin<sup>3,†</sup>, Yuliya Ya. Sokolova<sup>5</sup>, Kirill V. Mikhailov<sup>6,7</sup>, Vladimir V. Aleoshin<sup>6,7</sup> and Timur G. Simdyanov<sup>8</sup>

<sup>1</sup> Department of Invertebrate Zoology, Faculty of Biology, St Petersburg State University, St Petersburg, Russia

<sup>2</sup> Laboratory for Fauna and Systematics of Parasites, Center for Parasitology, Severtsov Institute of Ecology and Evolution, Russian Academy of Sciences, Moscow, Russian Federation

<sup>3</sup> Department of Botany and Zoology, Faculty of Science, Masaryk University, Brno, Czech Republic

<sup>4</sup> Centre Algatech, Institute of Microbiology of the Czech Academy of Sciences, Třeboň, Czech Republic

<sup>5</sup> Institute of Cytology, Russian Academy of Sciences, St Petersburg, Russian Federation

<sup>6</sup> Belozersky Institute for Physico-Chemical Biology, Lomonosov Moscow State University, Moscow, Russian Federation

<sup>7</sup> Kharkevich Institute for Information Transmission Problems, Russian Academy of Sciences, Moscow, Russian Federation

<sup>8</sup> Department of Invertebrate Zoology, Faculty of Biology, Lomonosov Moscow State University, Moscow, Russian Federation

† Deceased.

## ABSTRACT

**Background.** Gregarines are a major group of apicomplexan parasites of invertebrates. The gregarine classification is largely incomplete because it relies primarily on light microscopy, while electron microscopy and molecular data in the group are fragmentary and often do not overlap. A key characteristic in gregarine taxonomy is the structure and function of their attachment organelles (AOs). AOs have been commonly classified as “mucrons” or “epimerites” based on their association with other cellular traits such as septation. An alternative proposal focused on the AOs structure, functional role, and developmental fate has recently restricted the terms “mucron” to archigregarines and “epimerite” to eugregarines.

**Methods.** Light microscopy and scanning and transmission electron microscopy, molecular phylogenetic analyses of ribosomal RNA genes.

**Results.** We obtained the first data on fine morphology of aseptate eugregarines *Polyrhabdina pygospionis* and *Polyrhabdina cf. spionis*, the type species. We demonstrate that their AOs differ from the mucron in archigregarines and represent an epimerite structurally resembling that in other eugregarines examined using electron microscopy. We then used the concatenated ribosomal operon DNA sequences (SSU, 5.8S, and LSU rDNA) of *P. pygospionis* to explore the phylogeny of eugregarines with a resolution superior to SSU rDNA alone. The obtained phylogenies show that the *Polyrhabdina*

Submitted 16 December 2020

Accepted 14 July 2021

Published 16 September 2021

Corresponding author

Gita G. Paskerova,  
gitapasker@yahoo.com

Academic editor

Joseph Gillespie

Additional Information and  
Declarations can be found on  
page 24

DOI 10.7717/peerj.11912

© Copyright

2021 Paskerova et al.

Distributed under

Creative Commons CC-BY 4.0

OPEN ACCESS

clade represents an independent, deep-branching family in the Ancoroidea clade within eugregarines. Combined, these results lend strong support to the hypothesis that the epimerite is a synapomorphic innovation of eugregarines. Based on these findings, we resurrect the family Polyrhabdinidae [Kamm, 1922](#) and erect and diagnose the family Trollidiidae fam. n. within the superfamily Ancoroidea [Simdyanov et al., 2017](#). Additionally, we re-describe the characteristics of *P. pygospionis*, emend the diagnoses of the genus *Polyrhabdina*, the family Polyrhabdinidae, and the superfamily Ancoroidea.

**Subjects** Biodiversity, Molecular Biology, Parasitology, Taxonomy, Zoology

**Keywords** Eugregarinida, Intestinal parasites, Marine gregarines, Ultrastructure, SSU and LSU rDNA, Host-parasite relationships, Environmental DNA sequences, Phylogeny, Taxonomy

## INTRODUCTION

Apicomplexa are a large and diverse group of unicellular eukaryotes, many of which are symbionts of invertebrate and vertebrate animals ([Simdyanov et al., 2018](#)). Gregarines appear to be a monophyletic group of apicomplexan parasites—class Gregarinomorpha [Grassé, 1953](#) ([Janouškovec et al., 2019](#)). They are characterised by the pre-sexual association of gamonts (syzygy) and gametocyst production ([Simdyanov et al., 2017](#)). At present, gregarines include two groups: archigregarines (order Archigregarinida [Grassé, 1953](#)) which possess characters of plesiomorphic state and develop in the intestine of polychaetes and sipunculids, and eugregarines (order Eugregarinida [Léger, 1900](#)) which are parasites of the tissue, intestine and other cavities of diverse invertebrates ([Adl et al., 2019](#); [Desportes & Schrével, 2013](#); [Simdyanov et al., 2017](#)). Traditionally, gregarines also contained neogregarines, now a clearly polyphyletic mixture of eugregarines ([Cavalier-Smith, 2014](#); [Simdyanov et al., 2017](#)), and blastogregarines, which can be either considered as a separate class due to the lack of the gametocyst and syzygy ([Simdyanov et al., 2018](#)) or the sister group of archigregarines ([Janouškovec et al., 2019](#)). Eugregarines have been classified by the morphology of their dominant trophozoite and gamont stages into two groups. Septate eugregarines (Septata [Lankester, 1885](#)) have a fibrillar septum subdividing their cell into anterior and nucleated posterior parts and predominately parasitize terrestrial invertebrates. Aseptate eugregarines (Aseptata [Chakravarty, 1960](#)) lack the septum and inhabit mostly marine invertebrates ([Desportes & Schrével, 2013](#); [Simdyanov, 2007](#)). Molecular phylogenies show that this classification is not natural because septate eugregarines are polyphyletic ([Cavalier-Smith, 2014](#); [Simdyanov et al., 2017](#)).

Molecular phylogenetic studies of gregarines are limited by the availability of reference sequences and are largely based on small subunit (SSU) ribosomal DNA (rDNA) sequences (e.g., [Diakin et al., 2016](#); [Rueckert et al., 2018](#); [Wakeman & Leander, 2013](#); [Wakeman et al., 2017](#)). Since many gregarine SSU rDNA sequences form long branches in molecular phylogenies, both archi- and eugregarines were thought to be polyphyletic and possess characteristics of a convergent origin (e.g., [Cavalier-Smith, 2014](#)). However, recent studies that used the concatenated sequences of SSU and large subunit (LSU) rDNA genes have recovered relationships within Apicomplexa with a resolution superior to the analyses

inferred from SSU rDNA alone and revealed gregarines as monophyletic ([Paskerova et al., 2018](#); [Simdyanov, Diakin & Aleoshin, 2015](#); [Simdyanov et al., 2017](#); [Simdyanov et al., 2018](#)). This conclusion was unambiguously supported by phylogenetic analyses based on 296 ([Janouškovec et al., 2019](#)) and 195 ([Mathur, Wakeman & Keeling, 2021](#)) concatenated protein-coding genes. The observation that concatenated rDNA sequences perform better at resolving deep phylogenetic relationships in a group than SSU rDNA alone is receiving increasing support in studies of protist diversity ([Jamy et al., 2019](#)).

Most gregarines are extracellular parasites which attach with an attachment organelle (AO) to one or several host cells. The AO is commonly classified as “mucron” or “epimerite” depending on whether the gregarine is aseptate or septate, respectively ([Levine, 1971](#)). Reassessing the organization, function, and developmental fate of the AO in gregarine microscopy literature and in the aseptate eugregarine *Ancora sagittata* (Leuckart, 1860) Labbé, 1899, [Simdyanov et al. \(2017\)](#) proposed to restrict the term “epimerite” to the AO in eugregarines and the term “mucron” to the AO in archigregarines. The epimerite is an anchoring organelle, originated *de novo* in front of the trophozoite anterior end, varying in size and shape, and usually lost in the gamont. The mucron represents the hypertrophied anterior end of the trophozoite and gamont and is usually small, rounded or sucker-shaped.

In this study, we test the hypothesis that the epimerite is a synapomorphic trait of eugregarines. For this, we (1) studied the AO structure in the aseptate eugregarine *Polyrhabdina pygospionis* Caullery et Mesnil, 1914 parasitizing the polychaete *Pygospio elegans*; (2) compared fine morphology of *P. pygospionis* to that of *Polyrhabdina* cf. *spionis*, the type species from *Malacoceros fuliginosus*; and (3) resolved phylogenetic relationships of *P. pygospionis* with other groups of aseptate gregarines within the order Eugregarinida, using the analyses of sequences of concatenated ribosomal operon genes (SSU, 5.8S, and LSU rDNA). Our analyses revealed a new deep branching clade of aseptate eugregarines with the epimerite-type AO. This clade resurrects the family Polyrhabdinidae [Kamm, 1922](#) and belongs to the superfamily Ancoroidea [Simdyanov et al., 2017](#).

## MATERIALS & METHODS

### Collection of polychaete hosts and isolation of gregarines

Bristle worms *Pygospio elegans* Claparède, 1863 (Spionidae, Polychaeta) were collected at two sites of the littoral zone near the Marine Biological Station of St Petersburg State University (Bolshoy Goreliy Island, Keret' Archipelago, Chupa Inlet, Kandalaksha Bay, White Sea, 66°18.770'N; 33°37.715'E) and at the White Sea Biological Station of Lomonosov Moscow State University (Velikaja Salma strait, Kandalaksha Bay, White Sea, 66°33.200'N, 33°6.283'E) in the summer of 2002–2018. Polychaetes *Malacoceros fuliginosus* (Claparède, 1868) (Spionidae, Polychaeta) were collected under stones at the intertidal zone near the Roscoff Biological Station (English Channel, Atlantic Ocean, 48°43.652'N 3°59.285'W) in September 2010.

The examined animals were stored and dissected for isolation of parasites according to [Paskerova et al. \(2018\)](#). The released parasites or small fragments of the host intestine with attached gregarines were rinsed three times in seawater filtered through Millipore (0.22 µm), then fixed for electron microscopy.

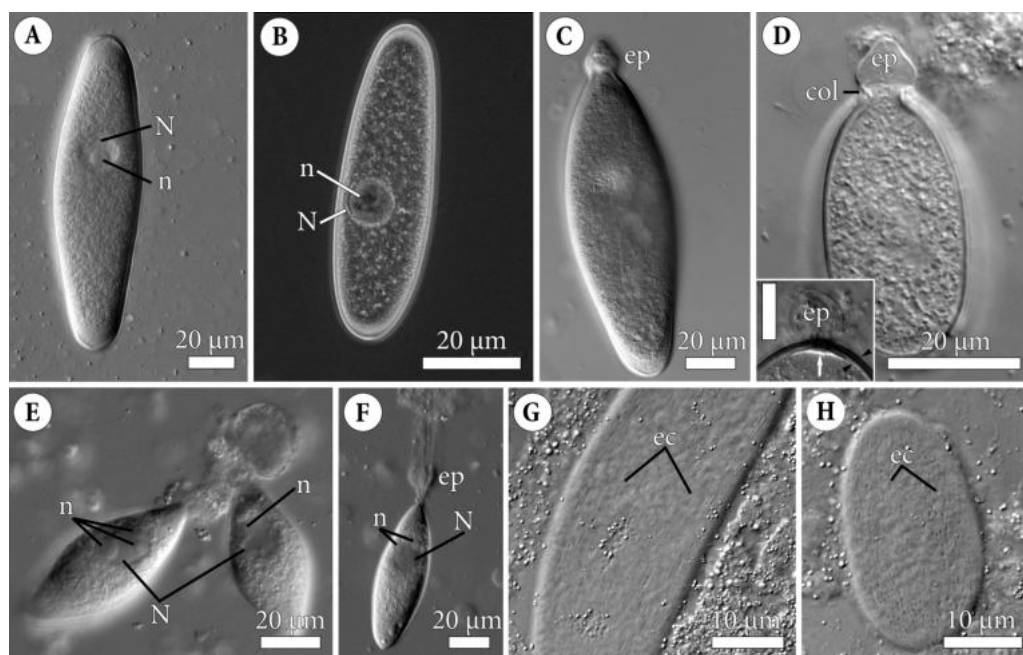


**Figure 1** General morphology of the eugregarine *Polyrrhabdina pygospionis*. Light differential interference (A, C–H) and phase contrast (B) microscopy. All micrographs show gregarines with the anterior end facing up. (A–B) Gamonts without the epimerite, slightly compressed with the coverslip; the nucleus (N) has one nucleolus (n). (C) Slightly compressed gamont with the epimerite (ep). (D) Compressed gamont with the epimerite (ep). Note the collar (col) surrounding the epimerite base. Inset. Another compressed gamont with a seal-like (white arrow) structure under the pellicle (between black arrowheads) in the zone of separation of the epimerite (ep, heavily compressed) from the cell; scale bar is 10 μm. (E) Two small gamonts glued to the host cell debris. Note nuclei (N) with three (left) and one (right) visible nucleoli (n). (F) Young trophozoite being mechanically dislodged from the host cell. Note long tensile cords deriving from the destroyed epimerite (ep), the nucleus (N) with two nucleoli (n). (G–H). Epicytic crests (ec) of compressed gamonts: almost straight (G, adjacent crests are mostly parallel or in apposition to each other) and undulated (H, many areas where adjacent crests are in opposition to each other).

Full-size [DOI: 10.7717/peerj.11912/fig-1](https://doi.org/10.7717/peerj.11912/fig-1)

## Light microscopy

More than 100 polychaetes of *P. elegans* were investigated in squash preparations with living parasites (Figs. 1A, 1D–1H). Separate eugregarines isolated from the host intestines were also investigated in living preparations (Figs. 1B–1C, Video S1). The microscopes used for observation were Leica DM2500 equipped with DIC optics, Plan-Apo objective lenses, and DFC 295 digital camera (Leica, Germany); MBR-1 (LOMO, Russia) equipped with phase contrast and Canon EOS 300D digital camera; Zeiss Axio Imager.A1 equipped with phase contrast and DIC optics and Axio-Cam MRC5 digital camera (Carl Zeiss, Germany). Maximal dimensions of gregarine cells were measured with the ImageJ program ([rsb.info.nih.gov/ij/](http://rsb.info.nih.gov/ij/)); average (av) and standard deviation (SD) values were calculated (Table S1).

## Electron microscopy

For scanning (SEM) and transmission (TEM) electron microscopy, small pieces of the polychaete intestine with attached eugregarines or free eugregarines released from the host

gut lumen were fixed in 2.5% glutaraldehyde in 0.2 M cacodylate buffer (pH 7.4, final osmolarity 720 mOsm) for 2 h, washed in filtered seawater and postfixed in 2% osmium tetroxide in the same buffer for 2 h (Figs. 2A–2H; 3A–3D; 4A–4D). For visualization of the glycocalyx and other mucosubstances, the samples were additionally fixed with 3% glutaraldehyde-ruthenium red [0.15% (w/v) stock water solution] in 0.2M cacodylate buffer (pH 7.4) and post-fixed with 1% OsO<sub>4</sub>-ruthenium red in the same buffer (Figs. 2I–2J; 3E–3G). Fixation was performed at +4°C. Fixed samples were dehydrated in an ascending ethanol series. For SEM, the fixed and dehydrated samples were critical point dried in liquid CO<sub>2</sub> and then coated with gold or platinum. The samples were investigated with GEMINI Zeiss Supra 40VP (Carl Zeiss, Germany) and JSM-7401F (JEOL, Japan) scanning electron microscopes. In total, more than 50 individuals of each species, *P. pygospionis* and *P. cf. spionis*, were examined by SEM. For TEM, samples of *P. pygospionis*, additionally dehydrated in an ethanol/acetone mixture and rinsed in pure acetone, were embedded in Epon-Araldite or Epon blocks. They were sectioned with ultramicrotomes Leica EM UC6 and Leica EM UC7 (Leica, Germany). Ultrathin sections were stained according to standard protocols and examined with LEO 910 (Carl Zeiss, Germany), JEM 2100 (JEOL, Japan), and JEM-1010 (JEOL, Japan) electron microscopes equipped with digital or film cameras. In total, more than 15 individuals of *P. pygospionis* were entirely sectioned and examined by TEM.

### **Polyrhabdina rRNAs assembly**

The rRNA of *P. pygospionis* was assembled from transcriptomic data generated from about 19 parasite cells isolated from five *P. elegans* polychaetes which were collected at Velikaya Salma strait, Kandalaksha Bay, White Sea, in 2016 (Janoušek *et al.*, 2019). Assembled, high-coverage transcripts corresponding to *P. pygospionis* ribosomal RNA were identified by BLASTN homology searches and joined at overlaps into eight larger contigs. Raw transcriptomic reads mapping onto the eight rRNA contigs were retrieved in Bowtie 2 (default settings) and used for extension of the contigs in Consed v29 with the following crossmatch parameters: -minmatch 50 -minscore 50 -penalty -9. Repeating this process in several iterations allowed us to merge and subsequently validate the complete rRNA operon sequence of *P. pygospionis* (comprising the SSU, ITS1, 5.8S, ITS2, and LSU). The final sequence was deposited into GenBank under the accession number MT214481.

We did not isolate DNA from *P. cf. spionis* cells because we found a limited number of cells, mostly of which were fixed for electron microscopy (see Results).

### **Molecular phylogenetic analysis**

The rDNA dataset for phylogenetic analyses was constructed using publicly available sequence data and designed to maximize the diversity of eugregarines at the family level. Unidentified environmental sequences and rDNA contigs from metagenome assemblies were found by BLAST searches (Altschul *et al.*, 1997) in the nr and wgs databases of NCBI. Small set of Coccidiomorpha (Coccidia and Hematozoa) species was used as an outgroup in the phylogenetic analyses.

Three datasets were prepared for phylogenetic analyses: taxonomically balanced SSU rDNA dataset (94 OTUs), a dataset without divergent long-branch OTUs (65 OTUs),

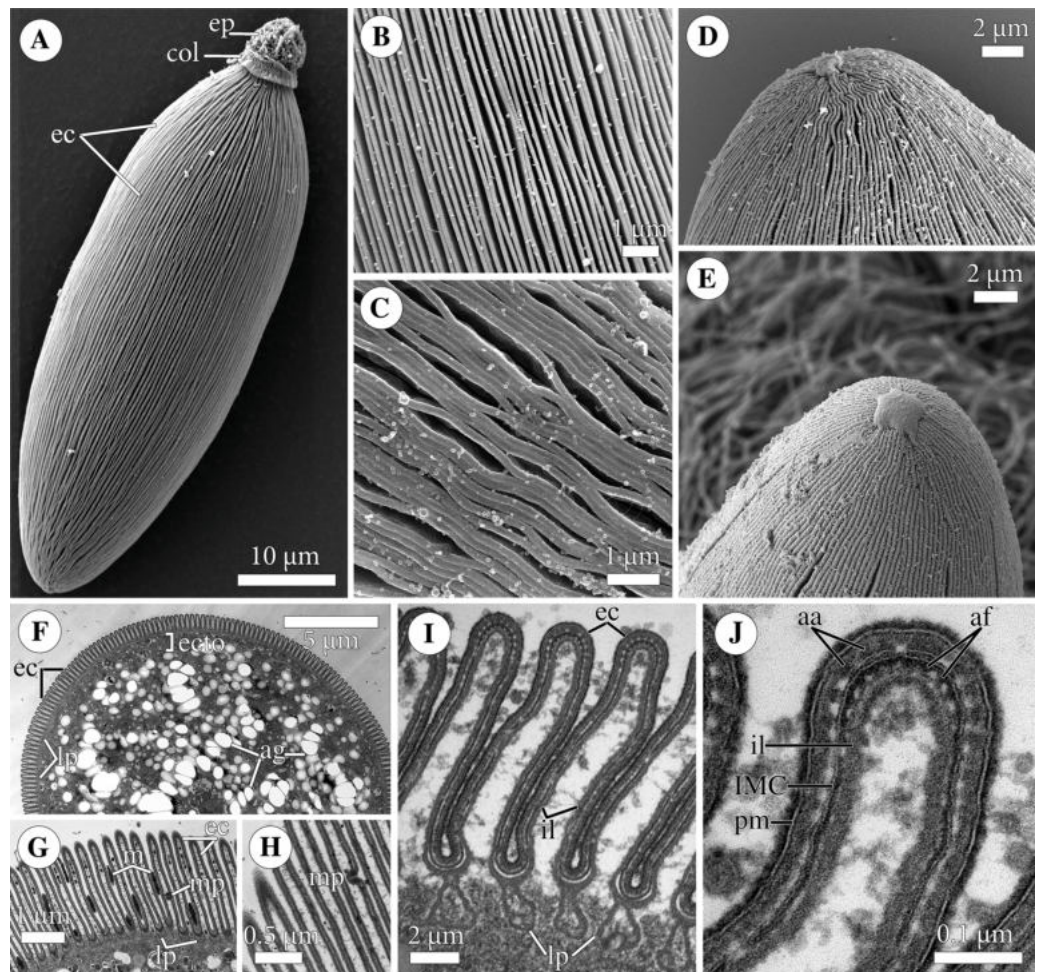


**Figure 2** Fine structure of the eugregarine *Polyrrhabdina pygospionis*. Scanning (A–E) and transmission (F–J) electron microscopy. (A) General morphology of a mechanically dislodged trophozoite with the epimerite (ep) having a collar (col) at the base and longitudinal epicytic crests (ec) on the cell surface. (B–C) Epicytic crests of two trophozoites at high magnification: B, almost straight; C, undulated. (D–E) The anterior end (D) and posterior end (E) of gamonts. Note the area where epicytic crests terminate. (F) Cross-section in the middle of a gamont showing epicytic crests (ec), loops of the internal lamina (lp) under the bottom of grooves between the epicytic crests, and differentiation of the ectoplasm (ecto) from the rest of the cytoplasm with amylopectin granules (ag). (G–H) Oblique sections of epicytic crests (ec). Note loops of the internal lamina (lp), a micropore (mp) on the wall of the epicytic crest, and presumably excreted mucous material (m) between crests. (I–J) Transversal section of finger-like epicytic crests (ec); J is a detail of I at a higher magnification. Note the three-membrane pellicle consisting of the plasma membrane (pm) covered by glycocalyx and the inner membrane complex (IMC) underlain by the internal lamina (il). In the apex of each crest, there are 10–12 apical rippled dense structures (aa) between the plasma membrane and IMC, and 10–12 apical filaments (af) under the IMC.

Full-size [DOI: 10.7717/peerj.11912/fig-2](https://doi.org/10.7717/peerj.11912/fig-2)

and a concatenated dataset with SSU, 5.8S, and LSU rDNA sequences (31 OTUs). The datasets were aligned in MUSCLE 3.6 (Edgar, 2004) and manually adjusted with BioEdit 7.0.9.0 (Hall, 1999): gaps, columns containing few nucleotides or hypervariable regions (V2, V4, V7, and V9) were removed, which resulted in 1,574-site (SSU) and 4,571-site (concatenated) alignments. To verify the results of manual masking, we additionally used

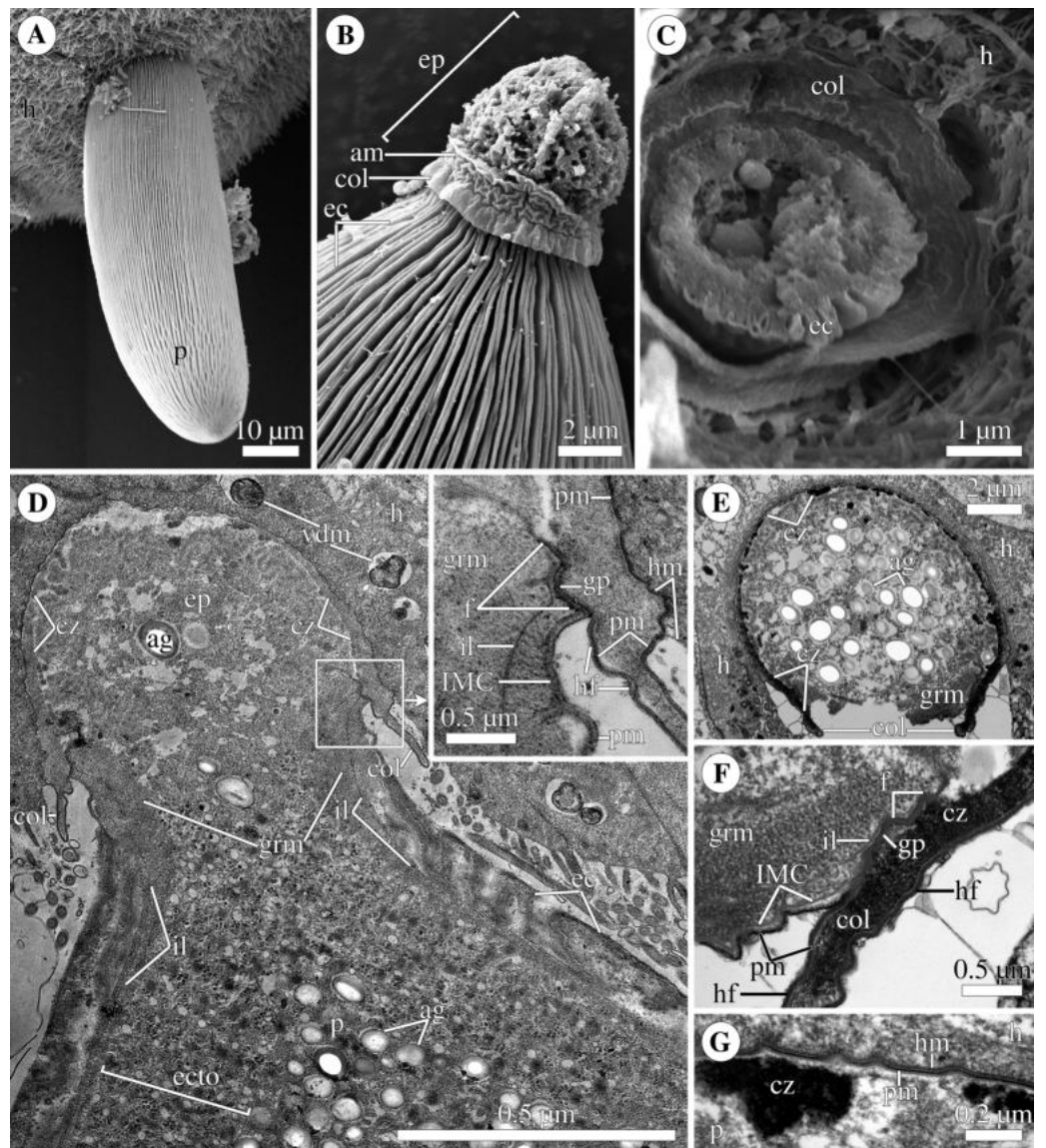


**Figure 3** Attachment organelle (epimerite) of the eugregarine *Polytrhabdina pygospionis*. Scanning (A–C) and transmission (D–G) electron microscopy. A. Trophozoite (p) embedded in a piece of the ciliated intestinal epithelium of the host (h). (B) Trophozoite (detail of Fig. 2A at a higher magnification) having the epimerite (ep) with a damaged apical surface membrane (am). Note longitudinal epicytic crests (ec) starting from under the collar (col) of the epimerite base. (C) Micrograph showing a broken off epimerite embedded in the host intestinal epithelium (h). Note epicytic crests (ec) and the collar (col) at the epimerite base. (D) Longitudinal section of a trophozoite (p), attached to the host cell (h) with the epimerite (ep), showing the differentiation of the peripheral cytoplasm into ectoplasm (ecto) poor in amylopectin granules (ag), epicytic crests (ec) starting from under the epimerite collar (col), internal lamina (il) under the gregarine pellicle, granular material (grm) of the ectoplasm at the epimerite base. Note the cortical zone (cz) of the epimerite filled with finely granular material. The infected host cell has vesicles with the material of heterogeneous electron density (vdm). Insert. A close up of part D at a higher magnification shows the terminal sections of the internal lamina (il) (continued on next page...)

Full-size  DOI: [10.7717/peerj.11912/fig-3](https://doi.org/10.7717/peerj.11912/fig-3)

**Figure 3 (...continued)**

and the inner membrane complex (IMC), the narrow and deep circular gap (gp) underlain by a fibrillar layer (f), the distal end of the circular host cell fold (hf) covering the collar and embedded in the gap. Note granular material (grm) with short fibrils mainly congregated near the termini of the internal lamina and IMC and a kind of tight cell junction between plasma membranes of the parasite AO (pm) and the host epithelial cell (hm). (E) Longitudinal section of an epimerite embedded into an invagination of the host cell (h). Note the collar (col) and granular material (grm) at the epimerite base, fine electron-dense granular material in the cortical zone (cz) and the cytoplasm filled with amylopectin granules (ag) in the middle of the epimerite. (F) Details of the epimerite collar (col) base. The cortical zone (cz) of the collar has fine electron-dense granular cytoplasm and is covered by the parasite plasma membrane (pm) and a thin circular host cell fold (hf), the distal end of which was embedded in the circular gap (gp) underlain by the fibrillar layer (f). Note the granular material (grm) and the termini of the internal lamina (il) and inner membrane complex (IMC). (G) Contact zone between the host (h) and parasite (p) cells. Note the host (hm) and parasite (pm) plasma membranes, and fine electron-dense granular material in the epimerite cortical zone (cz).

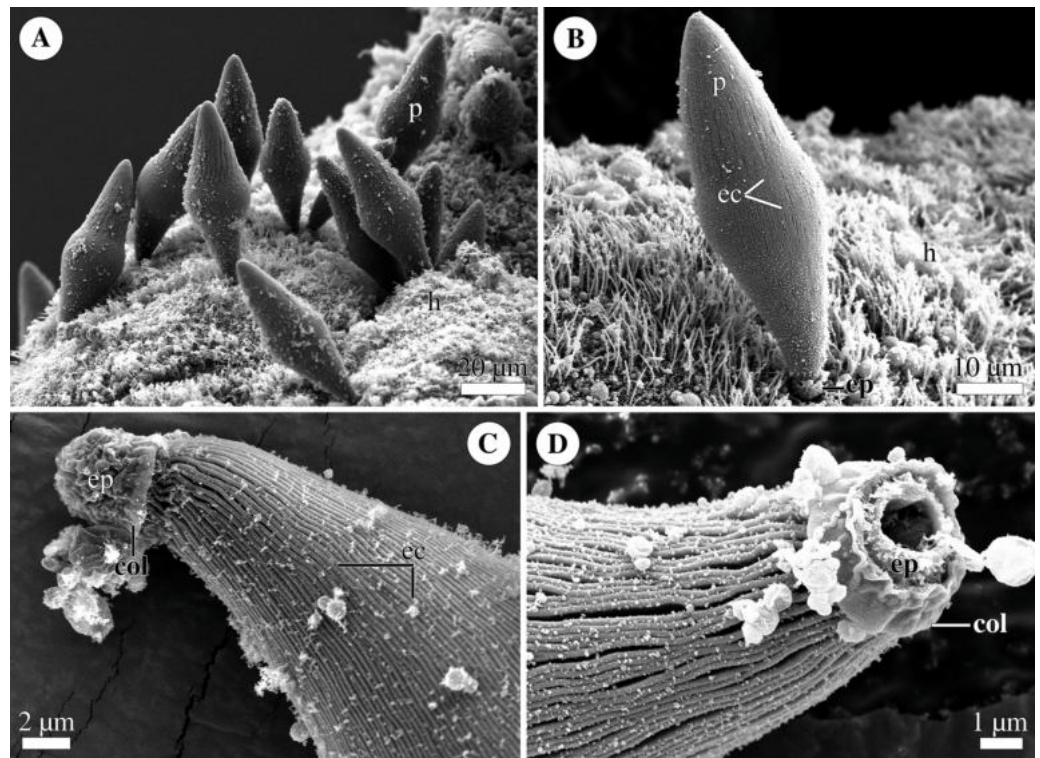


**Figure 4** General morphology of the eugregarine *Polyrrhabdina cf. spionis*. Scanning electron microscopy (A). Several trophozoites (p) attached to the host intestinal epithelium (h). (B) Attached trophozoite (p) with the epimerite (ep) partly embedded into the host intestinal epithelium (h) and longitudinal epicytic crests (ec). (C) Details of a detached trophozoite with the preserved epimerite. Note that longitudinal epicytic crests (ec) emerge from under the collar (col) at the base of the globular epimerite (ep). (D) Details of a mechanically dislodged trophozoite. The apical part of the epimerite (ep) embedded in the host cell was broken off, while the collar (col) at the epimerite base was retained.

Full-size [DOI: 10.7717/peerj.11912/fig-4](https://doi.org/10.7717/peerj.11912/fig-4)

two different automatic alignment and masking strategies for the SSU datasets. With the first strategy, the alignment of SSU rDNA sequences was done with MAFFT ([Katoh & Standley, 2013](#)) using a combination of local and structural alignments: the initial draft alignment was prepared using the local alignment with generalized affine gap cost (E-INS-i), the variable gap-rich regions were then aligned individually with the secondary structure aware alignment (X-INS-i) employing MXSCARNA ([Tabei et al., 2008](#)) to produce the final alignment. Prior to analyses the alignment was masked with trimAl ([Capella-Gutierrez, Silla-Martinez & Gabaldon, 2009](#)) using a gap threshold of 0.5 and a minimum block size of 3; the result was a 1,578-site alignment. The second strategy employed the GUIDANCE2 web server ([Landan & Graur, 2008](#); [Penn et al., 2010](#); [Sela et al., 2015](#)) and MAFFT (E-INS-i) to generate a series of alignments with varying confidence score thresholds. Columns with confidence scores below 0.715, 0.794, 0.900, 0.942, 0.970, 0.973, and 0.990 were removed resulting in 1,574, 1,471, 1,366, 1,257, 1,126, 1,087 and 828-site long alignments, respectively. To obtain a similar series for the alignment generated using the first strategy, we calculated site-specific evolutionary rates with IQ-TREE 2.1.2 ([Minh et al., 2020](#)) and performed stepwise removal of sites starting with the fastest category.

Maximum-likelihood (ML) analyses were performed with IQ-TREE 2.1.2 ([Minh et al., 2020](#)) using non-parametric bootstrap (-b 1000) and ultrafast bootstrap approximation (UFBoot, bb 1000) ([Minh, Nguyen & von Haeseler, 2013](#)) employing the CIPRES Science Gateway ([Miller, Pfeiffer & Schwartz, 2010](#)). Bayesian inference (BI) analyses were done with MrBayes 3.2.6 ([Ronquist et al., 2012](#)), PhyloBayes ([Lartillot et al., 2013](#)), and Phycas 2.2 ([Lewis, Holder & Swofford, 2015](#)). Evolutionary models for ML and Bayesian analyses were selected with ModelFinder ([Kalyaanamoorthy et al., 2017](#)): the GTR+F+I+G8 model was selected for the SSU rDNA datasets, and the SSU and LSU partitions in the concatenated dataset, while the GTR+F+G8 model was selected for the 5.8S partition. The following parameters of Metropolis Coupled Markov Chain Monte Carlo (mcmc) were used: nchains = 8, nruns = 2, temp = 0.025, ngen = 5,000,000, samplefreq = 1,000, burninfrac = 0.5. The average standard deviations of split frequencies at the end of BI (MrBayes) computations were 0.005044 for the 94 OTU dataset, 0.012636 for the 65 OTU dataset, and 0.003799 for the 31 OTU dataset. The ML support values were assigned to the SSU Bayesian tree using 1000 non-parametric bootstrap trees from the ML analysis *via* the -sup option of IQ-TREE 2.1.2 ([Minh et al., 2020](#)). Additional BI analysis of full manually masked SSU alignment (1,574 bp) was performed with PhyloBayes ([Lartillot et al., 2013](#)) under the GTR+ G8+CAT model (four chains, 20,000 cycles, the first half of sample points were discarded as burn-in). Constrained tree search and approximately unbiased (AU) tests were performed with IQ-TREE 2.1.2 ([Minh et al., 2020](#)).

Differences in the ML trees obtained with X-INS-i, GUIDANCE2 or full manually masked alignments were outlined by means of the principal component analysis (PCA). Using the bpcomp program of PhyloBayes, the ML trees were represented as sets of bipartitions with the corresponding bipartition support values treated as variables for PCA. For the analysis we used the support values calculated with UFBoot by IQ-TREE. The set of tree bipartitions used for PCA was reduced from the initial full set to just 146 bipartitions, representing only the interrelationships of main gregarine groups—groups

that were well-supported by all analyses. The PCA was performed using R (*R Core Team, 2021*) and R packages FactoMineR (*Lê, Josse & Husson, 2008*), factoextra, and ggplot2 (*Wickham, 2016*).

The secondary structure of helix 17 (numbering according to *Wuyts, Van de Peer & De Wachter, 2001*) of SSU rRNA was predicted using the Mfold server (*Zuker, 2003*) at <http://www.unafold.org/mfold/applications/rna-folding-form.php>.

### New zoological taxonomic names

The electronic version of this article in Portable Document Format (PDF) will represent a published work according to the International Commission on Zoological Nomenclature (ICZN), and hence the new names contained in the electronic version are effectively published under that Code from the electronic edition alone. This published work and the nomenclatural acts it contains have been registered in ZooBank, the online registration system for the ICZN. The ZooBank LSIDs (Life Science Identifiers) can be resolved and the associated information viewed through any standard web browser by appending the LSID to the prefix <http://zoobank.org/>. The LSID for this publication is: urn:lsid:zoobank.org:pub:693369E6-B319-4BB1-8E61-148FC4F5B271. The online version of this work is archived and available from the following digital repositories: PeerJ, PubMed Central SCIE and CLOCKSS.

## RESULTS

### *Polyrhabdina pygospionis*

#### Occurrence

Eugregarines *P. pygospionis* were found in the intestine of 126 out of 302 (42%) examined *Pygospio elegans* polychaetes (Spionidae). The intensity of infection usually varied from 1 to 50 (mode 1, average (av.) 6) gregarines per host. Parasites *P. pygospionis* co-occurred with other symbionts, archigregarines *Selenidium pygospionis* *Paskerova et al., 2018*, in the gut of 66 polychaetes (52%) versus 60 worms (48%) infected only by eugregarines. From the life cycle stages, trophozoites (attached eugregarines) and gamonts (non-attached eugregarines) were found in the host intestine.

#### General and fine structure

The cell shape of gamonts varied from ellipsoid sometimes slightly curved to pear-shaped. Gamonts were circular in cross section, with rounded anterior and posterior ends. No septum was observed (*Figs. 1A–1F, 2A, 2F; Table S1*). Gamonts had a large, oval or almost spherical nucleus positioned longitudinally in the widest part of the cell, usually closer to the anterior end. In large gamonts, one large spherical nucleolus was observed in the nucleus (*Figs. 1A–1B*). In small gamonts, two to four spherical nucleoli of diverse sizes were situated at opposing nuclear poles (*Figs. 1E–1F*). Gamonts moved by gliding without obvious changes in the cell shape (*Video S1*).

The cell surface of gamonts had numerous longitudinal epicytic crests (or folds; in this study, we use the terminology of *Simdyanov et al. (2017)*). They were almost straight (*Figs. 1G; 2A–2B*) or undulated (*Figs. 1H; 2C*). At the parasite ends, epicytic crests passed

into smooth areas, usually smaller at the anterior end and larger at the posterior one (Figs. 2D–2E). The cortex organization of the finger-like crests was typical of eugregarines: a three-membrane pellicle of 32–36 nm thick consisting of the plasma membrane and inner membrane complex (IMC). The pellicle was covered by a cell coat (glycocalyx) of about 10 nm and underlain by the internal lamina, an electron-dense fibrillar layer (Figs. 2F–2J). The internal lamina of 17–23 nm thick formed additional loops under the bottom of grooves between the epicytic crests. No links in the base of each crest were visible, due to which the crest cytoplasm communicates freely with the bulk of the cell cytoplasm (Figs. 2G, 2I). In the crest tip, there were 10–12 apical rippled dense structures (apical arcs) between the plasma membrane and the IMC as well as 10–12 apical 12-nm filaments under the IMC (Fig. 2J). Micropores typical for apicomplexans were present on lateral walls of epicytic crests (Figs. 2G–2H). Electron-dense material, presumably excreted mucus, was observed in between crests in some epicyte regions of parasite cells (Fig. 2G). In *Polyrhabdina* cells, the ectoplasm, a peripheral cytoplasm layer free of amylopectin, and the endoplasm, the bulk cytoplasm enriched with rounded amylopectin granules, were not distinctly separated (Fig. 2F). The thickness of the ectoplasm varied from 0.2 to 0.6  $\mu\text{m}$  in the middle cell region; anterior and posterior zones of ectoplasm were usually equally sized.

The trophozoites were anchored in the host intestinal epithelium by a dome-shaped AO (Figs. 3A–3C; Table S1). Rarely, this organelle was also observed in gamonts (Figs. 1C–1D). The AO in trophozoites was almost entirely embedded into a deep invagination of the host epithelial cell. A circular fold facing posteriorly—the collar—was presented at the base of the AO (Fig. 1D). This collar was located above the apical surface of the host cell and limited the area of AO insertion into the host cell invagination (Figs. 3B–3D). Epicytic crests started from the AO base under the collar (Fig. 3C). Trophozoites mechanically dislodged from the intestinal epithelium during material preparation had an AO with a damaged apical surface corresponding to the host-parasite attachment site (Fig. 3B). The intact AO was covered only by the parasite plasma membrane, and the IMC terminated at the AO base (Figs. 3D–3G). The attachment site had an appearance of a tight cell junction without a distinct gap between plasma membranes of the AO and host cell. Both membranes were underlain by electron-dense areas of fibrillar-like appearance (Figs. 3D–3G). The collar represented a thin extension of the AO and was covered by the parasite plasma membrane (Figs. 3D–3F, 3D, 3F). The cytoplasm of the AO was distinctly differentiated into two zones: a finely granular cortical zone located peripherally under the plasma membrane and within the collar, and a vesicular zone positioned in the centre and having occasional organelles typical for the rest of the parasite body, e.g., amylopectin granules (Figs. 3D, 3E). The infected host cell formed a thin circular fold at its apical surface. This fold consisted of two closely adjacent plasma membranes almost without any cytoplasm in between them and tightly surrounded the epimerite collar of the attached parasite (Fig. 3D). The distal end of the host circular fold was embedded in a gap of about 45 nm width and 600 nm depth located circularly at the base of the parasite AO under the collar. In the parasite cytoplasm, this circular gap was underlain by a fibrillar layer - the endpoint of the IMC. The terminus of the internal lamina was located under this layer (Figs. 3D inset, 3F). The ectoplasm

of this region contained granular material with short fibrils mainly congregated near the termini of the internal lamina and IMC (Figs. 3D–3F).

According to our observation on living *P. pygospionis* cells, during mechanical AO separation from the parasite cell, the edges of the anterior end seem to be pulled together and sometimes only a small part of the cytoplasm escaped (Video S1). The wound surface was probably sealed by the granular cytoplasm with short fibrils located in the AO base (Fig. 1D inset; Fig. S1A). The fine structure of the anterior end of recently detached gamonts corresponded to our *in vivo* observations (Fig. S1B). In some parasites mechanically separated from the host cell by the pressure of a coverslip, long tensile cords were derived from the epimerite cytoplasm and the underlying ectoplasm (Fig. 1F). Basing on these obtained data, we presume that *P. pygospionis* gamonts usually discard their epimerites and, as a result, detach from the host tissue.

All parasitized host cells had an altered appearance: near the host-parasite contact zone, they had electron-dense, organelle-depleted cytoplasm with vesicles containing material of heterogeneous electron density, sometimes surrounded by an additional membrane (Fig. 3D). This may be considered as a host response to the gregarine infection.

Some examined eugregarines *P. pygospionis* were infected with microsporidia *Metchnikovella incurvata* Caullery and Mesnil, 1914 and *M. spiralis* Sokolova *et al.*, 2014 (Figures S1A–S1B). Interestingly, these microsporidia also occupied the AO of infected gregarines (not shown).

### ***Polyrhabdina cf. spionis* (Von Kölliker, 1845) Mingazzini, 1891** **Occurrence**

Eugregarines *P. cf. spionis* were found in the intestine of 3 out of 18 (17%) *Malacoceros fuliginosus* polychaetes (Spionidae). One worm was relatively heavily infected, about 50 parasites per host, while others had only several eugregarines. From the life cycle stages, mainly trophozoites were found in the host intestine.

### **General morphology**

Trophozoites were spindle- or rhomboid-shaped, wide in the cell middle and with a rounded posterior end (Fig. 4A; Table S1). A single rounded nucleus was in the widest part of the cell (not shown). Trophozoites were anchored in the intestinal epithelium by a globular AO with the collar around its base (Figs. 4B–4D). In some individuals, the collar was located above the apical surface of the host cell (Fig. 4A). The cell surface of parasites was covered with longitudinal epicytic crests, straight or slightly undulated. Epicytic crests started from the AO base under the collar (Fig. 4B). The parasites moved by gliding (not shown).

### **Phylogenies inferred from rDNA sequences**

SSU rDNA phylogenies inferred by the Bayesian inference (BI) in MrBayes (Fig. 5) and Phycas and by the Maximum-likelihood (ML) analyses (not shown) using the full manually masked alignment showed almost identical topologies with a few minor differences. In both phylogenies, the sequence of *Polyrhabdina pygospionis* was placed in a robustly supported clade of 23 environmental sequences derived from marine sediments and one

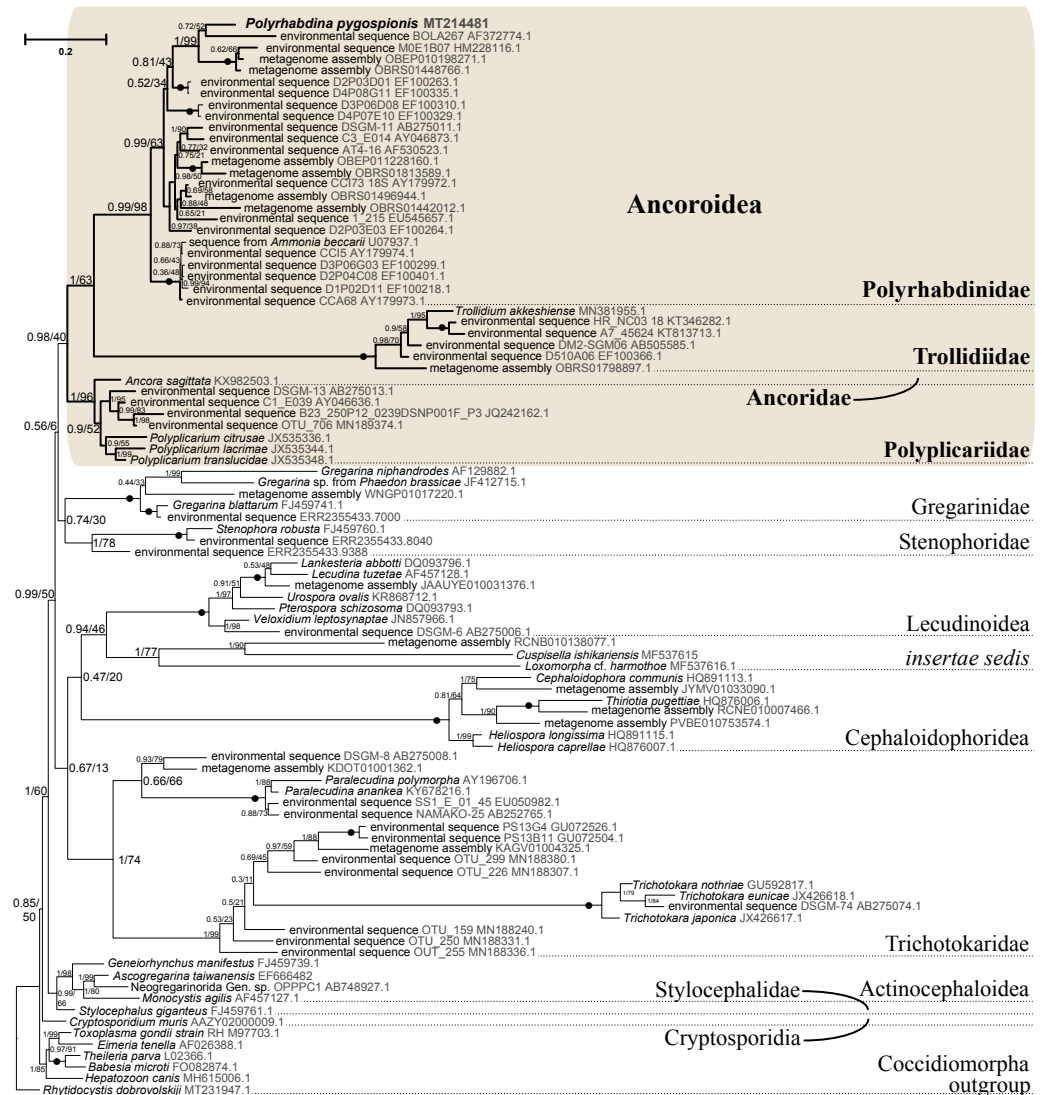


**Figure 5** Bayesian tree of eugregarines inferred from the manually masked dataset of 94 SSU rDNA sequences and 1,574 sites under the GTR+F+I+G8 model. Numbers at branches indicate Bayesian posterior probabilities (numerator) and ML bootstrap percentage (denominator). Black dots on the branches indicate Bayesian posterior probabilities and bootstrap percentages of 1.0 and 100%, respectively. The newly obtained sequence of *Polyrrhabdina pygospionis* is in bold. The names of major eugregarine lineages correspond to *Simdyanov et al., 2017* and *Cavalier-Smith, 2014*.

Full-size DOI: 10.7717/peerj.11912/fig-5

sequence derived from the foraminiferan *Ammonia beccarii* (see Discussion). This clade is subdivided into two subclades and is grouped with a clade consisting of *Trollidium akkeshiense* and five environmental sequences with high posterior probability (PP = 1.0) but low non-parametric bootstrap percentage (BP = 63%) supports. A clade containing *Ancora sagittata* and *Polyrrhabdina* species appears sister to the group with *Polyrrhabdina* and *Trollidium* with statistically significant PP = 0.98, but low BP = 40%. BI analysis performed in PhyloBayes shows the same composition of Ancoroidea, but alternative

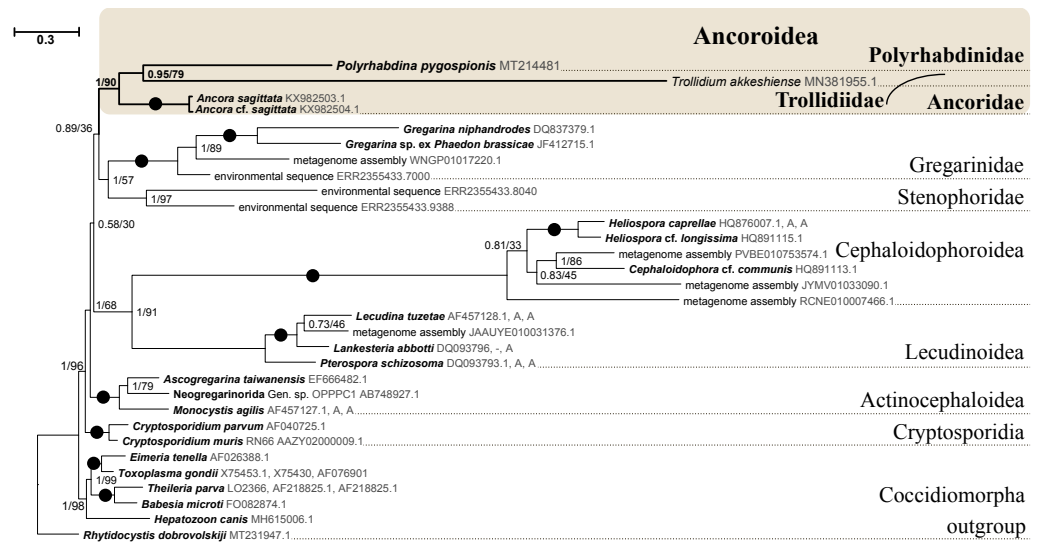


**Figure 6** Bayesian inference tree of eugregarines obtained from the manually masked dataset of 31 concatenated SSU, 5.8S, and LSU rDNA sequences (4,571 sites). Designations are the same as in Fig. 5. Full-size [DOI: 10.7717/peerj.11912/fig-6](https://doi.org/10.7717/peerj.11912/fig-6)

topology with rearrangement of subclades within Polyrrhabdinidae (Fig. S2). The analyses of the concatenated dataset (SSU rDNA+5.8S rDNA+ LSU rDNA) improved the resolution of the tree (Fig. 6), however, the taxonomic sampling was reduced and the phylogenetic diversity of gregarines was lower (see Materials and Methods). The position of *P. pygospionis* did not change in this tree: it was still a sister taxon to *Trollidium* with moderate support (PP = 0.95, BP = 79%). Importantly, the *Trollidium*-*Polyrrhabdina* and *Ancora* dichotomy received stronger support as well (PP = 1, BP = 90%). Judging by the result of BI and the ML analyses, *Polyrrhabdina* and relatives are presumably members of the superfamily Ancoroidea (see Discussion).

The Ancoroidea clade uniting *Polyrrhabdina pygospionis*, *Trollidium akkeshiense*, *Ancora sagittata*, *Polyplicarium* spp., and related environmental sequences is consistently present in the ML trees based on the dataset constructed using structural alignment (X-INS-i) as well as with the derivative alignments after sequential deletion of rapidly evolving sites, supporting the results obtained with manually masked alignments (Fig. S3). However, these phylogenies are generally in disagreement with the results obtained with the GUIDANCE2 alignments, which were generated with varying confidence score thresholds (Fig. S3). The GUIDANCE2 trees show less reconciliation in the topology and composition of subclades for the Ancoroidea, which usually involve the clade of *Trichotokara* and *Paralecudina*, but not necessarily *Trollidium*. Close relationship of the *Trichotokara* + *Paralecudina* clade with Ancoroidea is also observed with the manually masked dataset if CAT model of molecular evolution implemented in PhyloBayes program is applied (Fig. S3) or the most divergent sequences are excluded (65 OTUs) (Fig. S4). In an attempt to resolve the discrepancy between the results of structural alignment and GUIDANCE2 experiments, we tested the possible composition of the Ancoroidea. We built constrained trees with four

different subclade sets (including or excluding *Trollidium*, *Trichotokara* and *Paralecudina*, and *Cephaloidophora*) for full and 1471-site alignments generated with GUIDANCE2 and structural alignment, and performed AU tests (Table S2). The AU tests did not reject the tested alternatives at the 5% significance level, although the *p*-values were highly dependent on the alignment used. We also performed the PCA for resolving main differences in topologies generated using three different alignment and masking strategies (Fig. S5). These differences were in Ancoroidea composition and *Trichotokara* + *Paralecudina* clade position, and some other systematic differences with a smaller contribution for these series of topologies. However, the PCA showed a preference for manual strategies as the obtained trees were more stable (red dots formed a denser group than green or blue ones in the data matrix, Fig. S5).

A shared feature of most Polyrrhabdinidae, *Trollidium*, and related environmental sequences was found in the predicted structure of helix 17 of the SSU rRNA (numbering according Wuyts, Van de Peer & De Wachter, 2001). In most of these OTUs, the 3'-strand of helix 17 contains an additional nucleotide, forming a second bulge in the helix, while the typical state for eukaryotes is a single 1-nucleotide bulge in the 3'-strand (Fig. S6). No similar structures of helix 17 have been found outside Polyrrhabdinidae, *Trollidium*, and related environmental sequences, however, within the group the helix 17 is not constant and evolves along the phylogenetic tree. This feature is an additional evidence for *Polyrrhabdina*-*Trollidium* relationships as the additional bulge in helix 17 was not included in any of the alignments used in this research.

## DISCUSSION

### ***Polyrrhabdina* species and their taxonomic position**

The genus *Polyrrhabdina* (original spelling *Polyrrabdina*) was established by Mingazzini (1891) with *Gregarina spionis* Kölliker, 1848, a gregarine isolated from the polychaetes *Scolecopsis fuliginosa* (Claparède, 1868) (now *Malacoceros fuliginosa*), as the type species. This genus was assigned to the family Lecudinidae Kamm, 1922 (Clopton, 2000; Ganapati, 1946; Grassé, 1953; Levine, 1971; Levine, 1977; Reichenow, 1929; Rueckert et al., 2018) or the family Polyrrhabdinidae Kamm, 1922 (Desportes & Schrével, 2013; Kamm, 1922) depending on the emphasis given to gregarine septation and, correspondingly, AO naming—mucron or epimerite.

To date, the genus *Polyrrhabdina* includes seven named species. One species has no description—*Polyrrhabdina* sp. from *Dipolydora socialis*. All known *Polyrrhabdina* spp. occur in the intestine of spionid polychaetes. All these species have been studied only using light and, in some cases, scanning electron microscopy (Caullery & Mesnil, 1897a; Caullery & Mesnil, 1897b; Caullery & Mesnil, 1914a; Caullery & Mesnil, 1919; Von Kölliker, 1845; Von Kölliker, 1848; Mingazzini, 1891; Reichenow, 1932; Mackinnon & Ray, 1931; Ganapati, 1946; Kamm, 1922; Fowell, 1936; De Faria, De Cunha & Da Fonseca, 1918; Rueckert et al., 2018; Table S3). No molecular sequence data are available for *Polyrrhabdina* except for two sequences published in Rueckert et al. (2018), which are currently retracted from GenBank to clarify potential fungal contamination (Dr. Rueckert, pers. comm., 2020).

In *Polyrhabdina* spp., the only life cycle stages that have ever been described are the trophozoite, usually with a globular AO embedded in the host epithelium, and the gamont that usually lost its AO during separation from the host tissue. In trophozoites, some authors observed hook-like processes on the apical AO surface in addition to a circllet of tiny prongs (“teeth”) at its base (Caullery & Mesnil, 1914a; Ganapati, 1946; Von Kölliker, 1848; Mackinnon & Ray, 1931; Reichenow, 1932; Rueckert et al., 2018). In contrast, others described the AO with a collar, a posteriorly oriented circular fold, at its base and sometimes with a ring of small prongs, anterior to the collar (Fowell, 1936; Léger, 1893; Mackinnon & Ray, 1931). There was no consensus in these works on calling the AO a mucron or epimerite (Table S3).

Caullery and Mesnil recorded the eugregarine *Polyrhabdina pygospionis* in polychaetes *Pygospio seticornis* (now *P. elegans*) from the English Channel but did not provide an adequate description of this species. The host name and the infection caused by microsporidia *Metchnikovella incurvata* and *M. oviformis* are available evidence from this species (Caullery & Mesnil, 1914a; Caullery & Mesnil, 1914b; Caullery & Mesnil, 1919). We believe that we collected namely eugregarines *P. pygospionis* in the White Sea because they parasitized *P. elegans* polychaetes and were found to be infected by the microsporidium *M. incurvata* (Paskerova et al., 2016; Rotari, Paskerova & Sokolova, 2015; Sokolova et al., 2013)—in these articles, this gregarine is called *Polyrhabdina* sp.). Our transmission electron microscopic study of this eugregarine revealed peculiarities of the pellicle structure: the presence of loops of the internal lamina under epicytic grooves, which is not typical for eugregarines, and the absence of the internal lamina links at the epicytic crest bases, which is characteristic of some aseptate and septate eugregarines, e.g., *Ancora* and *Stylocephalus* (Desportes, 1969; Simdyanov, 1995; Simdyanov et al., 2017). Moreover, the AO of this gregarine is constructed as the epimerite of other studied eugregarines (see below). Based on the light, scanning and transmission electron microscopic data obtained in this study, we amend the diagnosis for *P. pygospionis* (see Taxonomic summary).

Eugregarines *P. spionis* and *P. bifurcata* (Mackinnon & Ray, 1931; Reichenow, 1932) were isolated from the polychaete *Scolelepis fuliginosa* (Claparède, 1868) (now *Malacoceros fuliginosus*). They were considered to be either variants of the same species *P. spionis* (Mackinnon & Ray, 1931) or separate species (Reichenow, 1932) distinguished by the number and morphology of prongs on the AO surface (Table S1). *P. spionis* has the epimerite with seven-nine bifurcated apical prongs, while *P. bifurcata* - with two large claw-like apical processes and a basal circllet of 14–16 min prongs. According to previously published drawings, the gregarines that we isolated from the polychaetes *Malacoceros fuliginosus* were more similar to *P. spionis* in appearance. Presumably, we observed young trophozoites of *P. spionis* judging from their reported cell sizes (Caullery & Mesnil, 1914a; Mackinnon & Ray, 1931; Reichenow, 1932; Table S3). Since we did not study the ultrastructure of *Polyrhabdina* cf. *spionis*, we cannot discuss the presence of prongs on the AO surface. Additionally, a collar at the AO base that we observed in *P. pygospionis* and *P. cf. spionis* has also been described in *P. polydora* (Caullery & Mesnil, 1914a; Kamm, 1922; Mackinnon & Ray, 1931; Fowell, 1936).

On the base of the superficial morphology of *P. pygospionis* and *P. cf. spionis*, the type species, and data on the fine structure of AO and cortex in *P. pygospionis*, we emend the diagnosis of the genus *Polyrhabdina* (see Taxonomy summary).

*Kamm (1922)* established the family Polyrhabdinidae for genera *Polyrhabdina*, *Sycia* Léger 1892, and *Ulivina* *Mingazzini, 1891* uniting septate eugregarines with the epimerite-type AO. The species composition of these genera is still not defined because their morphological characteristics are insufficient and overlapping. The only species, *S. inopinata* Léger 1891, has been investigated by transmission electron microscopy. *Sycia* spp. and *Ulivina* spp. occur mostly in the Cirratulidae and Eunicidae polychaetes (*Desportes & Schrével, 2013; Schrével, 1969; Schrével & Vivier, 1966*).

Similar to *Polyrhabdina* spp., an area of light, non-granulated cytoplasm in the cell under the AO was revealed in *Sycia* and *Ulivina* eugregarines by light microscopic studies. However, neither our electron microscopic data on *Polyrhabdina pygospionis*, nor the data on the fine structure of *S. inopinata* confirm the presence of a fibrillar septum dividing the gregarine cell into the anterior and nucleated posterior parts, as characteristic of true septate eugregarines (*Desportes & Schrével, 2013; Ganapati, 1946; Kamm, 1922; Mingazzini, 1891; Schrével, 1969; Schrével & Vivier, 1966*; present study).

In gregarines of these genera, AOs vary from a small papilla with or without a long filament at the apex in *Ulivina* spp. to a large rounded papilla with a thick collar (“ring”) around the base in *Sycia* spp. The figures of *S. inopinata* in *Schrével & Vivier (1966)* and *Schrével (1969)*, as well as personal communications of Prof. Schrével, allow suggesting that the collar is covered by the three-membrane pellicle and that the IMC terminates above the collar, but not under it as in *P. pygospionis*. Presumably, the collar of *S. inopinata* is a circular protrusion of the eugregarine cell under the globular AO. In addition, the granular cytoplasm with short fibrils in the AO base in *P. pygospionis* may correspond to a sphincter ring described in the AO in *S. inopinata*. In comparison with the pellicle of *P. pygospionis*, links of the internal lamina in the base of the epicytic crest as well as loops of the internal lamina under the bottom of epicytic grooves were apparently absent in *S. inopinata* (*Desportes & Schrével, 2013; Schrével, 1969; Schrével & Vivier, 1966*).

Due to scarce morphological and missing molecular data, the genera *Sycia* and *Ulivina* remain to be revised, and their relationships with *Polyrhabdina* need to be proved.

### **Epimerite is a shared characteristic of eugregarines**

The fine structure of attachment organelles was investigated in archigregarines *Selenidium* spp., aseptate eugregarines *Ancora sagittata*, *Difficilina cerebratuli*, *Lankesteria levinei*, *Lecudina* spp., and septate gregarines *Didymophyes gigantea*, *Epicavus araeoceri*, *Gregarina* spp., *Leidyana ephestiae*, *Pyxinia firmus*, *Stylocephalus africanus*. A revision of these data (*Simdyanov et al., 2017*) revealed conspicuous differences between the attachment organelles of archigregarines and eugregarines and proposed to restrict the term “epimerite” to the AO in eugregarines, but the term “mucron” to the AO in archigregarines. The epimerite is an anchoring organelle, which varies in size and shape, and it is sometimes equipped with projections. It is usually embedded in the host cell invagination and bordered by a circular gap which runs around the AO base and pinches a small portion of

the host cell. The epimerite is covered only by the plasma membrane, while the IMC of the pellicle terminates close to the circular gap at the epimerite base. Between the epimerite and infected host cell, a kind of tight cell junction is apparently formed. It may facilitate feeding by transmembrane transport. In trophozoites during their transformation from the zoite, the epimerite originates as a new organelle in front of their anterior end, with the simultaneous disappearance of some organelles of the apical complex characteristic of the zoite. As trophozoites develop into gamonts and detach from the host cell, they can lose the epimerite. In contrast, the mucron is usually small, rounded or sucker-shaped. It represents the hypertrophic developed anterior end of the zoite and performs feeding by using its well-developed apical complex as a cytostome-cytopharyngeal gateway for the myzocytosis - the feeding by sucking. The mucron persists in trophozoites and gamonts, and even at the syzygy stage. The recently obtained results on the fine structure of blastogregarines are in good agreement with the proposed hypothesis: blastogregarines, which share some plesiomorphic characters of archigregarines, possess the AO of similar structure and function of the mucron ([Simdyanov et al., 2018](#)).

According to our results, the AO of two *Polyrhabdina* spp. is organized in the same way as epimerites of other previously studied aseptate and septate eugregarines ([Fig. 7](#)). It represents an anchoring organelle covered only by the plasma membrane forming a kind of tight cell junction with the host cell membrane, and can be lost in gamonts. The evidence obtained in this study strongly corroborates the suggestion, that the epimerite is a shared, derived character (synapomorphy) of all eugregarines, both septate and aseptate, while the mucron is an intrinsic feature of archigregarines and blastogregarines—sporozoans preserving the apicomplexan zoite structure at the trophozoite and gamont stages ([Simdyanov et al., 2017](#); [Simdyanov et al., 2018](#)). This revised view on AO homology is in agreement with the recently emended diagnosis of Eugregarinida ([Simdyanov et al., 2017](#)).

### **The resurrected family Polyrhabdinidae and the emended superfamily Ancoroidea**

Molecular phylogenetic analyses of ribosomal RNA genes (SSU, 5.8S, and LSU rDNA) show that *P. pygospionis* typifies a large lineage of environmental eukaryotic sequences from marine sediments, which was previously shown to be related to Ancoroidea and designated as *incertae sedis* among gregarines ([Simdyanov et al., 2017](#)). Additionally, the recent protein multigene phylogeny also revealed the affiliation of *P. pygospionis* (*Polyrhabdina* sp. in original) with Ancoroidea ([Janoušková et al., 2019](#); [Mathur, Wakeman & Keeling, 2021](#)). We conclude that the clade including *P. pygospionis* can be identified as the family Polyrhabdinidae [Kamm, 1922](#), a taxon that should be re-established with a diagnosis emended by new morphological evidence (see Taxonomic summary). The two subclades identified in our phylogenetic analysis in the clade Polyrhabdinidae may correspond to *Polyrhabdina*, *Sycia* and/or *Ulivina* genera, but this needs to be further investigated.

Geographical mapping of the polyrhabdinid environmental samples reveals their worldwide distribution: deep sea sediment from the East Sea ([Park et al., 2008](#)), sediment from seashores of Denmark ([Karst et al., 2018](#)), sediment of mangrove system in Brazil

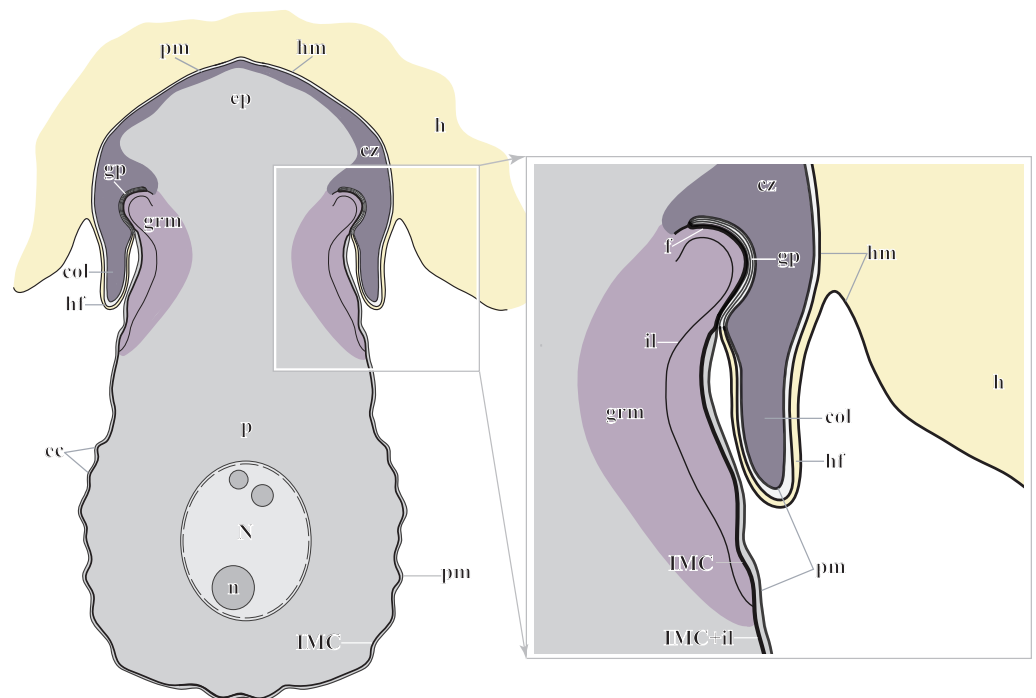


**Figure 7** Diagram of the trophozoite structure of the eugregarine *Polyrrhabdina pygospionis* attached to the host cell (not to scale). Abbreviations: col, epimerite collar; cz, cortical zone of epimerite cytoplasm; ec, epicytic crests; ep, epimerite; f, fibrillar layer; gp, circular gap at the epimerite base under the collar; grm, granular material of the ectoplasma; h, host cell; hf, host cell circular fold; hm, host plasma membrane; il, internal lamina of the parasite pellicle; IMC, inner membrane complex of the parasite pellicle; N, nucleus; n, nucleolus; p, parasite cell; pm, parasite plasma membrane.

Full-size DOI: 10.7717/peerj.11912/fig-7

(Santos *et al.*, 2010), methane cold seep in Sagami Bay in Japan, the tidal flat on Disko Island near Greenland, Cariaco basin in the Caribbean Sea near Venezuela, marine stromatolites near the Bahamas (Baumgartner *et al.*, 2009; Stoeck, Taylor & Epstein, 2003; Stoeck *et al.*, 2007; Takishita *et al.*, 2007), and a clone derived from the foraminiferan *Ammonia beccarii* (Wray *et al.*, 1995). The identification of the latter sequence as a foraminiferan was refuted (Pawlowski *et al.*, 1996), and it probably originated by either pseudoparasitism, occasional ingestion of a gregarine oocysts by the foraminiferan (see Rueckert *et al.* (2011) for similar cases of misidentification).

SSU + LSU rDNA phylogeny, SSU rDNA phylogenies built with alternative alignment procedures, and the BI analysis performed in PhyloBayes confirm the placement of *Trollidium akkeshiense* within the Ancoroidea. In addition, most *Trollidium*, Polyrrhabdinidae, and related environmental sequences share an unusual feature in the predicted secondary structure of helix 17 of the SSU rRNA that might indicate their common ancestry. Earlier, helix 17 was identified as a phylogenetic marker of some metazoan and protistan clades (Aleshin *et al.*, 1998; Nikolaev *et al.*, 2004). The clade associated with *T. akkeshiense* and several related environmental sequences was previously assigned to the family Lecudinidae (Rueckert & Leander, 2010; Rueckert, Wakeman &

*Leander, 2013; Wakeman, 2020*). Following the criteria established in earlier taxonomic revisions of gregarines based on rDNA phylogenies (*Clopton, 2009; Cavalier-Smith, 2014; Paskerova et al., 2018; Simdyanov et al., 2017*), we erect the SSU rDNA clade, typified by *T. akkeshiense*, as a new family Trollidiidae (see Taxonomic summary). GUIDANCE2 alignment tends to place the *Trichotokara+Paralecudina* clade in the Ancoroidea, while the manually masked alignment brings these groups closer together only if using a BI under the CAT model (PhyloBayes tree), which is most free from the artifact of long branch attraction, or if excluding the most divergent sequences from the alignment (65 OUT tree). This is consistent with a recent multigene analysis of *Trichotokara* as a sister group to Ancoroidea (*Mathur, Wakeman & Keeling, 2021*). Generally, the GUIDANCE2 strategy showed less stable results than the structural alignment utilizing the X-INS-i algorithm, in particular with regard to placement of the *Trichotokara* and *Paralecudina* clade as well as the *Cephaloidophora* and Trollidiidae clades. The PCA result also showed that fully manual constructed alignments gave more stable results than the other two automatic alignments. The rDNA data offers method-dependent resolution for the composition of the Ancoroidea, and the results require further refinement. Currently, we propose that the superfamily Ancoroidea combines four families: Ancoridae *Simdyanov et al., 2017*, Polyplicariidae *Cavalier-Smith, 2014*, Polyrrhabdinidae *Kamm, 1922, emend.*, and Trollidiidae fam. nov. Characteristics of these groups are given in Taxonomic summary.

### **Candidate synapomorphies of the family Polyrrhabdinidae and the emended superfamily Ancoroidea**

Comparative analysis of the ultrastructural data and reconciling those with the molecular phylogenies allow us to detect additional candidate synapomorphies of Polyrrhabdinidae and Ancoroidea.

In the attached eugregarines *P. pygospionis* and *P. cf. spionis*, almost the whole epimerite is embedded into the host cell, except for the collar, which is located above the surface of the host cell. The collar appears to be a shared characteristic of the genus *Polyrrhabdina* and possibly also of the family Polyrrhabdinidae, provided that the relationship of *Sycia* with this family is confirmed. The epimerite and its collar may provide a scaffold for formation of projections and prongs for better attachment to the host cell.

A shared characteristic among many gregarines that make up the clade Ancoroidea is a well-developed protruded epimerite detected in *Ancora* (family Ancoridae *Simdyanov et al., 2017*), *Polyplicarium* (Polyplicariidae *Cavalier-Smith, 2014*), *Polyrrhabdina* (Polyrrhabdinidae *Kamm, 1922, emend.*) (*Cavalier-Smith, 2014; Cecconi, 1905; Simdyanov et al., 2017; Wakeman & Leander, 2013; this study*). The epimerite is usually lost in parasites detached from the host cell. In place of the lost epimerite (discarded or retracted), a residual structure may be retained, e.g., a disk-shaped protrusion (“mucron” in original) observed in *Trollidium akkeshiense* (*Wakeman, 2020*).

Another shared characteristic and a candidate synapomorphy of the superfamily Ancoroidea is likely the absence of the links of the internal lamina in between the bases of the epicytic crests (*Fig. 2I*). Apart from *P. pygospionis*, the links are absent in *Ancora sagittata* (*Simdyanov et al., 2017*) and, re-examining pictures in the original studies, most

likely also in *Trollidium akkeshiense* (Wakeman, 2020: Fig. 12), and in *Sycia inopinata* (Schrével, 1969: Fig. 23), a presumable member of the superfamily. Septate gregarines of the genus *Stylocephalus* (Desportes, 1969; Desportes & Schrével, 2013) also lack the links but are not related to Ancoroidea (Fig. 5), indicating that the two taxa acquired similar epicyte structure by convergent loss of the internal lamina links.

It is possible that the superfamily Ancoroidea includes other known species of marine gregarines. The eugregarines *Kamptocephalus mobilis* Simdyanov, 1995 and *Mastigorhynchus bradae* Simdyanov, 1995, parasitizing flabelligerid polychaetes, resemble *T. akkeshiense* by the fine structure of the epicyte and by the type of motility (Simdyanov, 1995; Wakeman, 2020). All these gregarines have wide epicytic crest without links of the internal lamina in their base and possess a well-developed epimerite, which is usually absent in gamonts. In addition, *K. mobilis* shows both intermittent bending of the anterior third of the body and fast gliding, and has a massive bundle of longitudinal microtubules in the subpellicular cytoplasm (Simdyanov, 1995). Hence, *K. mobilis* and *M. bradae* have all the features of *Trollidium* and ancoroids in general, but their affiliation is yet to be confirmed by molecular analyses.

### Notes on gregarine co-parasitism and microsporidian hyperparasitism in polychaetes

Eugregarines *Polyrhabdina* species often co-occur with archigregarines *Selenidium* species in the same polychaete host (Table S3). Our observations suggest that in co-infection of *P. pygospionis* and *S. pygospionis* in *Pygospio elegans* (Paskerova et al., 2018; this study) each parasite species is more abundant than in monoinfections. Eugregarines, blastogregarines, and archigregarines regularly harbour metchnikovellid microsporidia (Caullery & Mesnil, 1897a; Caullery & Mesnil, 1897b; Caullery & Mesnil, 1919; Ganapati, 1946; Mackinnon & Ray, 1931; Mikhailov et al., 2021; Paskerova et al., 2016; Paskerova et al., 2018; Rotari, Paskerova & Sokolova, 2015; Sokolova et al., 2013; Sokolova et al., 2014; Table S3). Further studies focused on metchnikovellids that infect gregarines co-occurring in the same spionid polychaete may shed some light on the diversification of metchnikovellids and co-evolution of gregarine hosts and their hyperparasitic microsporidia.

### Taxonomic summary

Phylum Apicomplexa Levine, 1970

Subphylum Sporozoa Leuckart, 1879

Class Gregarinomorpha Grassé, 1953, emend. Simdyanov et al., 2017

**Order Eugregarinida** Léger, 1900, emend. Simdyanov et al., 2017.

**Superfamily Ancoroidea** Simdyanov et al., 2017, emend.

**Diagnosis.** Eugregarinida. Typically aseptate; trophozoites typically with prominent epimerite; epimerite lost in gamonts; micropores on lateral walls of epicytic crests lacking the links of the internal lamina in their bases. In polychaetes, intestine.

**Type family.** Ancoridae Simdyanov et al., 2017.

**Remarks.** Four families. The superfamily may be supplemented with parasites of Flabelligeridae polychaetes, *Kamptocephalus mobilis* Simdyanov, 1995, *Mastigorhynchus bradae* Simdyanov, 1995, which share the characteristics of the epicyte structure and motility with those of ancoroids (see Discussion). The affiliation of these gregarines with this superfamily needs to be tested.

**Family Polyrrhabdinidae** Kamm, 1922, emend.

**Diagnosis.** Ancoroidea. Trophozoites and gamonts ovoid, aseptate; epimerite massive, with various appendages: prongs and/or basal collar (posteriorly oriented circular fold at the epimerite base). Intestine of polychaetes.

**Type genus.** *Polyrrhabdina* Mingazzini, 1891.

**Remarks.** One to three genera. *Sycia* and *Ulivina* species have non-granulated cytoplasm in the cell body under the epimerite, which gives their appearance of septate cells. The validity and composition of these genera and its close relations to *Polyrrhabdina* and other ancoroid eugregarines must be clarified.

**Genus *Polyrrhabdina*** Mingazzini, 1891, emend.

**Diagnosis.** Polyrrhabdinidae. Trophozoites and gamonts aseptate. Intestine of Spionidae.

**Type species.** *Polyrrhabdina spionis* (Kölliker, 1848) Mingazzini, 1891.

**Remarks.** Seven named species.

***Polyrrhabdina pygospionis*** Caullery and Mesnil, 1914, emend.

**Original description.** *Polyrrhabdina pygospionis*, n. sp., from *Pygospio seticornis* (now *P. elegans*) (Caullery & Mesnil, 1914a). Infected by microsporidia *Metchnikovella incurvata* Caullery et Mesnil, 1914 and *M. oviformis* Caullery et Mesnil, 1914 (Caullery & Mesnil, 1914b; Caullery & Mesnil, 1919). Gregarines generally abundant in the polychaete intestine, similar to *P. brasili* Caullery et Mesnil, 1914 from *Spio martinensis* Mesnil, 1896 but smaller (Caullery & Mesnil, 1919).

**Re-description (amended diagnosis).** Characteristics of the genus. Trophozoites and gamonts ellipsoid (sometimes slightly curved) to pear-shaped, circular in cross section, 28–288 × 14–50 μm. Nucleus oval to spherical, 9.5–19.0 × 9.5–17.0 μm, oriented longitudinally in the widest part of the cell, with single large or 2–3 small nucleoli of various localization. Epimerite domed, 3.7–4.9 μm in base diameter, with a posteriorly oriented circular fold (collar), 0.2–1.7 μm tall, and an annular narrow and deep gap at the base; lost (presumably discarded) in gamonts of different sizes. Epicytic crests (about 5/μm) with 10–12 apical rippled dense structures and 10–12 apical filaments in the tops. Other stages not found. Infected by different metchnikovellidean microsporidia.

**Type locality.** Anse Saint-Martin, English Channel, North East Atlantic.

**Type definitive host.** *Pygospio elegans* (former *P. seticornis*) Claparède, 1863 (Polychaeta, Spionidae).

**Locality and host used in amended diagnosis.** Kandalaksha Bay, White Sea; *Pygospio elegans* Claparède, 1863 (Polychaeta, Spionidae).

**Ecology/Habitat.** Marine.

**Type materials.** Lost.

**Deposition of specimens and materials used in amended diagnosis.** Resin blocks and fixed slides containing eugregarines and pieces of infected host intestine deposited in the

collection of Department of Invertebrate Zoology, St Petersburg State University; [Figs. 1–3](#) (this publication) show some of these specimens (White Sea). DNA sequences: contiguous sequence of SSU, ITS1, 5.8S, ITS2, and LSU rDNA from the individuals, isolated from the polychaetes *Pygospio elegans* (Kandalaksha Bay, White Sea) (GenBank accession number MT214481).

**Family Trollidiidae fam. nov.**

**Diagnosis.** Ancoroidea. Free individuals (putatively gamonts; epimerite unknown) with extraordinarily wide longitudinal epicytic crests, some crests zigzag; the network of longitudinal microtubules in cortex under the zigzag epicytic crests; bending/twitching motility. Intestine of Flabelligeridae. Monotypic.

**Type genus.** *Trollidium* [Wakeman, 2020](#).

**ZooBank Registration:** LSID urn:lsid:zoobank.org:pub:693369E6-B319-4BB1-8E61-148FC4F5B271. **ZooBank Nomenclature Act:** LSID urn:lsid:zoobank.org:act:239658AC-6AE9-4641-B2F3-E18FE5616363.

**Remarks.** The family may be supplemented with other parasites of Flabelligeridae polychaetes, *Kamptocephalus mobilis* [Simdyanov, 1995](#) and *Mastigorhynchus bradae* [Simdyanov, 1995](#), which share with *Trollidium* the characteristics of the epicyte structure and motility (see Discussion). The affiliation of these gregarines with this family needs to be tested.

## CONCLUSIONS

On the base of comprehensive study, we re-described the aseptate eugregarine *Polyrhabdina pygospionis* Caullery, Mesnil, 1914 from the polychaete *Pygospio elegans*, collected in the White Sea. We also demonstrated that the attachment organelles of *P. pygospionis* and *P. cf. spionis*, the type species, represented the epimerite in its organization. This evidence once again proves that the epimerite is an innovation of eugregarines. The phylogenetic analyses using concatenated ribosomal operon DNA sequences revealed that *P. pygospionis* was not related to lecudinooid eugregarines (the superfamily Lecudinoidea [Simdyanov et al., 2017](#)), but to ancoroid eugregarines (the superfamily Ancoroidea [Simdyanov et al., 2017](#)). Based on the results of ribosomal phylogenetic analysis and comparative analysis of the literature data, we revised the superfamily Ancoroidea and proposed the following synapomorphies for this group: the well-developed protruded epimerite usually missing in gregarines detached from the host cell and the absence of the links of the internal lamina joining the base of the epicytic crests. Accordingly, the superfamily unites four families: Ancoridae ([Simdyanov et al., 2017](#)), Polyplacariidae ([Cavalier-Smith, 2014](#)), Polyrhabdinidae [Kamm, 1922](#), emend., and Trollidiidae fam. nov.

## ACKNOWLEDGEMENTS

The authors would like to thank the staff of the Marine Biological Station of St Petersburg State University, the White Sea Biological Station of Moscow State University for providing facilities for field sampling and material processing. GGP is grateful to Professor Rudolf Entzeroth and Markus Gunther (Technical University of Dresden) for providing facilities

for her research. GGP and TSM utilized equipment of the core facility centers of St Petersburg State University: “Molecular and Cell Technologies” for electron microscopy and “Observatory of Environmental Safety” for culturing of marine invertebrates. AV and MK are grateful to the Laboratory of Electron Microscopy, Biology Centre CAS, an institution supported by the Czech-BioImaging large RI project (LM2015062 funded by MEYS CR), for their help with obtaining some EM data. TGS utilized equipment of the Electron Microscopy Laboratory of the Faculty of Biology and the Center of Microscopy of the White Sea Biological Station, Lomonosov Moscow State University. To make computations, the CIPRES Science Gateway (*Miller, Pfeiffer & Schwartz, 2010*) was used in this study. The research was carried out as part of the scientific project of the state order of the government of Russian Federation to Lomonosov Moscow State University No.121032300117-3.

## ADDITIONAL INFORMATION AND DECLARATIONS

### Funding

The phylogenetic analysis and scanning electron microscopy were supported by the Russian Science Foundation (project number 18-04-00123); fieldworks and transmission electron microscopy were supported by the Russian Foundation for Basic Research (grant numbers 18-04-00324, 18-04-01359) and the Czech Science Foundation (project number GBP505/12/G112 (ECIP – Centre of excellence)). The funders had no role in study design, data collection and analysis, decision to publish, or preparation of the manuscript.

### Grant Disclosures

The following grant information was disclosed by the authors:

The Russian Science Foundation: project number 18-04-00123.

The Russian Foundation for Basic Research: 18-04-00324, 18-04-01359.

The Czech Science Foundation (project number GBP505/12/G112 (ECIP – Centre of excellence)).

### Competing Interests

The authors declare there are no competing interests.

### Author Contributions

- Gita G. Paskerova conceived and designed the experiments, performed the experiments, analyzed the data, prepared figures and/or tables, authored or reviewed drafts of the paper, contributed to the material collection and processing, wrote the paper, and approved the final draft.
- Tatiana S. Miroljubova, Andrea Valigurová and Vladimir V. Aleoshin conceived and designed the experiments, performed the experiments, analyzed the data, prepared figures and/or tables, authored or reviewed drafts of the paper, contributed to the material collection and processing, and approved the final draft.

- Jan Janouškovec and Kirill V. Mikhailov conceived and designed the experiments, performed the experiments, analyzed the data, authored or reviewed drafts of the paper, contributed to the material collection and processing, and approved the final draft.
- Magdaléna Kováčiková and Yuliya Ya. Sokolova performed the experiments, analyzed the data, prepared figures and/or tables, authored or reviewed drafts of the paper, contributed to the material collection and processing, and approved the final draft.
- Andrei Diakin performed the experiments, prepared figures and/or tables, contributed to the material collection and processing, and approved the final draft.
- Timur G. Simdyanov conceived and designed the experiments, performed the experiments, analyzed the data, prepared figures and/or tables, authored or reviewed drafts of the paper, contributed to the material collection and processing, wrote the paper, and approved the final draft.

### DNA Deposition

The following information was supplied regarding the deposition of DNA sequences:

The complete rRNA operon sequence (comprising the SSU, ITS1, 5.8S, ITS2, and LSU) of *Polyrhabdina pygospionis* is available in the [Supplementary File](#).

### Data Availability

The following information was supplied regarding data availability:

All raw measurements and calculations are available in the [Supplementary File](#).

Resin blocks and fixed slides containing eugregarines and pieces of infected host intestine deposited in the collection of the Department of Invertebrate Zoology, St Petersburg State University (accession numbers 3-6, 622-623, 678-680, 734, 786, 794-795, 862, 879 in the section “*Polyrhabdina pygospionis*”; accession numbers 742-743 in the section “*Polyrhabdina cf. spionis*”).

### New Species Registration

The following information was supplied regarding the registration of a newly described species:

Publication LSID: urn:lsid:zoobank.org:pub:693369E6-B319-4BB1-8E61-148FC4F5B271

Trollidiidae fam. nov.: urn:lsid:zoobank.org:act:239658AC-6AE9-4641-B2F3-E18FE5616363.

### Supplemental Information

Supplemental information for this article can be found online at <http://dx.doi.org/10.7717/peerj.11912#supplemental-information>.

## REFERENCES

- Adl SM, Bass D, Lane CE, Lukeš J, Schoch CL, Smirnov A, Agatha S, Berney C, Brown MW, Burki F, Cárdenas P. 2019. Revisions to the classification, nomenclature, and diversity of eukaryotes. *Journal of Eukaryotic Microbiology* **66**(1):4–119 DOI 10.1111/jeu.12691.

- Aleshin VV, Kedrova OS, Milyutina IA, Vladychenskaya NS, Petrov NB. 1998.** Secondary structure of some elements of 18S rRNA suggests that stronglylid and a part of rhabditid nematodes are monophyletic. *FEBS Letters* **429**:4–8 DOI [10.1016/S0014-5793\(98\)00550-X](https://doi.org/10.1016/S0014-5793(98)00550-X).
- Altschul SF, Madden TL, Schäffer AA, Zhang J, Zhang Z, Miller W, Lipman DJ. 1997.** Gapped BLAST and PSI-BLAST: a new generation of protein database search programs. *Nucleic Acids Research* **25**(17):3389–3402 DOI [10.1093/nar/25.17.3389](https://doi.org/10.1093/nar/25.17.3389).
- Baumgartner LK, Spear JR, Buckley DH, Pace NR, Reid RP, Dupraz C, Visscher PT. 2009.** Microbial diversity in modern marine stromatolites, Highborne Cay, Bahamas. *Environmental Microbiology* **11**(10):2710–2719 DOI [10.1111/j.1462-2920.2009.01998.x](https://doi.org/10.1111/j.1462-2920.2009.01998.x).
- Capella-Gutierrez S, Silla-Martinez JM, Gabaldon T. 2009.** trimAl: a tool for automated alignment trimming in large-scale phylogenetic analyses. *Bioinformatics* **25**:1972–1973 DOI [10.1093/bioinformatics/btp348](https://doi.org/10.1093/bioinformatics/btp348).
- Caullery M, Mesnil F. 1897a.** Sur un type nouveau (*Metchnikovella* n.g.) d'organismes parasites des grégarines. *Comptes Rendus Hebdomadaires de Séances et Mémoires de la Société de Biologie* **49**:960–962.
- Caullery M, Mesnil F. 1897b.** Sur trois sporozoaires parasites de la *Capitella capitata* O.Fab. *Comptes Rendus Hebdomadaires de Séances et Mémoires de la Société de Biologie* **49**:1005–1008.
- Caullery M, Mesnil F. 1914a.** Sur l'existence de grégarines dicystidées chez les annélides polychètes. *Comptes Rendus Hebdomadaires de Séances et Mémoires de la Société de Biologie* **77**:516–520.
- Caullery M, Mesnil F. 1914b.** Sur les Metchnikovellidae et autres protistes parasites des grégarines d'annélides. *Comptes Rendus Hebdomadaires de Séances et Mémoires de la Société de Biologie* **77**:527–532.
- Caullery M, Mesnil F. 1919.** Metschnikovellidae et autres protistes parasites des Gregarines d'Annelides. *Annales de l'Institut Pasteur* **33**(4):209–240.
- Cavalier-Smith T. 2014.** Gregarine site-heterogeneous 18S rDNA trees, revision of gregarine higher classification, and the evolutionary diversification of Sporozoa. *European Journal of Protistology* **50**(5):472–495 DOI [10.1016/j.ejop.2014.07.002](https://doi.org/10.1016/j.ejop.2014.07.002).
- Cecconi J. 1905.** Sur l' *Anchorina sagittata* Leuck. parasite de la *Capitella capitata* O. Fabr. *Archiv für Protistenkunde* **6**:230–244.
- Clopton R. 2000.** Order Eugregarinorida Léger, 1900. In: Lee JJ, Leedale GF, Bradbury F, eds. *An illustrated guide to the protozoa: organisms traditionally referred to as protozoa, or newly discovered groups*. Vol. 1. Lawrence: Society of Protozoologists, 205–298.
- Clopton RE. 2009.** Phylogenetic relationships, evolution, and systematic revision of the septate gregarines (Apicomplexa: Eugregarinorida: Septatorina). *Comparative Parasitology* **76**(2):167–190 DOI [10.1654/4388.1](https://doi.org/10.1654/4388.1).
- Desportes I. 1969.** Ultrastructure et développement des Grégarines du genre *Stylocephalus*. *Annales des Sciences Naturelles. Zoologie et Biologie Animale* **11**:31–96.
- Desportes I, Schrével J (eds.) 2013.** Treatise on zoology—anatomy, taxonomy, biology. In: *The gregarines (2 vols). The early branching apicomplexa*. Boston: Brill Leiden.

- Diakin A, Paskerova GG, Simdyanov TG, Aleoshin VV, Valigurová A. 2016.** Morphology and molecular phylogeny of coelomic gregarines (Apicomplexa) with different types of motility: *Urospora ovalis* and *U. trivisiae* from the polychaete *Trivisia forbesii*. *Protist* **167**:279–301 DOI [10.1016/j.protis.2016.05.001](https://doi.org/10.1016/j.protis.2016.05.001).
- Edgar RC. 2004.** MUSCLE: multiple sequence alignment with high accuracy and high throughput. *Nucleic Acids Research* **35**:1792–1797.
- De Faria G, De Cunha M, Da Fonseca OR. 1918.** Protozoários parasitos de *Polydora socialis*. *Memorias do Instituto Oswaldo Cruz* **10**:17–19 DOI [10.1590/S0074-02761918000100002](https://doi.org/10.1590/S0074-02761918000100002).
- Fowell RR. 1936.** Observations on the Sporozoa inhabiting the gut of the polychaete worm *Polydora flava* Claparède. *Parasitology* **28**:414–430 DOI [10.1017/S0031182000022599](https://doi.org/10.1017/S0031182000022599).
- Ganapati PN. 1946.** Notes on some gregarines from polychaetes of the Madras coast. *Proceedings of the Indian Academy of Sciences. Section B, Biological Sciences* **23**(5):228–248.
- Grassé PP. 1953.** Classe des gregarinomorphes (Gregarinomorpha n. nov.; Gregarinae Haeckel, 1866; Gregarinidea Lankester, 1885; gregarines des auteurs). Vol. 1. Paris: Masson & Cie, 550–690.
- Hall TA. 1999.** BioEdit: a user-friendly biological sequence alignment editor and analysis program for Windows 95/98/NT. *Nucleic Acids Symposium Series* **41**:95–98.
- Jamy M, Foster R, Barbera P, Czech L, Kozlov A, Stamatakis A, Bending G, Hilton S, Bass D, Burki F. 2019.** Long-read metabarcoding of the eukaryotic rDNA operon to phylogenetically and taxonomically resolve environmental diversity. *Molecular Ecology Resources* **20**(2):429–443 DOI [10.1111/1755-0998.13117](https://doi.org/10.1111/1755-0998.13117).
- Janouškovec J, Paskerova GG, Miroljubova TS, Mikhailov KV, Birley T, Aleoshin VV, Simdyanov TG. 2019.** Apicomplexan-like parasites are polyphyletic and widely but selectively dependent on cryptic plastid organelles. *eLife* **8**:e49662 DOI [10.7554/eLife.49662](https://doi.org/10.7554/eLife.49662).
- Kalyaanamoorthy S, Minh BQ, Wong TKF, Von Haeseler A, Jermiin LS. 2017.** ModelFinder: fast model selection for accurate phylogenetic estimates. *Nature Methods* **14**:587–589 DOI [10.1038/nmeth.4285](https://doi.org/10.1038/nmeth.4285).
- Kamm WM. 1922.** Studies on gregarinines II. Synopsis of the polycystid gregarines of the world, excluding those from the Myriapoda, Orthoptera, and Coleoptera. *Illinois Biological Monographs* **VII**(1):1–103.
- Karst S, Dueholm M, McIlroy S, Kirkegaard RH, Nielsen PH, Albertsen M. 2018.** Retrieval of a million high-quality, full-length microbial 16S and 18S rRNA gene sequences without primer bias. *Nature Biotechnology* **36**(2):190–195 DOI [10.1038/nbt.4045](https://doi.org/10.1038/nbt.4045).
- Katoh K, Standley DM. 2013.** MAFFT multiple sequence alignment software version 7: improvements in performance and usability. *Molecular Biology and Evolution* **30**:772–780 DOI [10.1093/molbev/mst010](https://doi.org/10.1093/molbev/mst010).
- Landan G, Graur D. 2008.** Local reliability measures from sets of co-optimal multiple sequence alignments. *Pacific Symposium on Biocomputing* **13**:15–24.

- Lartillot N, Rodrigue N, Stubbs D, Richer J. 2013.** PhyloBayes MPI: phylogenetic reconstruction with infinite mixtures of profiles in a parallel environment. *Systematic Biology* **62**:611–615 DOI [10.1093/sysbio/syt022](https://doi.org/10.1093/sysbio/syt022).
- Lê S, Josse J, Husson F. 2008.** FactoMineR: an R package for multivariate analysis. *Journal of Statistical Software* **25**:1–18.
- Léger L. 1893.** L'évolution des gregarines intestinales des vers marins. *Comptes Rendus de l'Académie des Sciences* **116**:204–206.
- Levine ND. 1971.** Uniform terminology for the protozoan subphylum Apicomplexa. *Journal of Protozoology* **18**(2):352–355 DOI [10.1111/j.1550-7408.1971.tb03330.x](https://doi.org/10.1111/j.1550-7408.1971.tb03330.x).
- Levine ND. 1977.** Revision and checklist of the species (other than *Lecudina*) of the aseptate gregarine family Lecudinidae. *Journal of Protozoology* **24**(1):41–52 DOI [10.1111/j.1550-7408.1977.tb05279.x](https://doi.org/10.1111/j.1550-7408.1977.tb05279.x).
- Lewis PO, Holder MT, Swofford DL. 2015.** Phycas: software for Bayesian phylogenetic analysis. *Systematic Biology* **64**:525–531 DOI [10.1093/sysbio/syu132](https://doi.org/10.1093/sysbio/syu132).
- Mackinnon DL, Ray HN. 1931.** Observations on dicystid gregarines from marine worms. *Quarterly Journal of Microscopical Science* **74**:439–466.
- Mathur V, Wakeman K, Keeling P. 2021.** Parallel functional reduction in the mitochondria of apicomplexan parasites. *Current Biology* **31**(13):2920–2928 DOI [10.1016/j.cub.2021.04.028](https://doi.org/10.1016/j.cub.2021.04.028).
- Mikhailov KV, Nasonova ES, Shishkin YA, Paskerova GG, Simdyanov TG, Yudina VA, Smirnov AV, Janoušková J, Aleoshin VV. 2021.** Ribosomal RNA of the metchnikovellids in gregarine transcriptomes and rDNA of the microsporidia sensu lato in environmental metagenomes. *Zhurnal Obshchei Biologii* **82**(3):201–228 DOI [10.31857/S0044459621030040](https://doi.org/10.31857/S0044459621030040).
- Miller MA, Pfeiffer W, Schwartz T. 2010.** Creating the CIPRES science gateway for inference of large phylogenetic trees. In: *Gateway computing environments workshop (GCE)*. New Orleans, LA, 1–8.
- Mingazzini P. 1891.** Gregarine monocistidee, and conosciute, nuove poco and del Golfo di Napoli. *Atti Reale Accad. Lincei. Rendiconti* **7**:229–235.
- Minh BQ, Nguyen MAT, Von Haeseler A. 2013.** Ultrafast approximation for phylogenetic bootstrap. *Molecular Biology and Evolution* **30**:1188–1195 DOI [10.1093/molbev/mst024](https://doi.org/10.1093/molbev/mst024).
- Minh BQ, Schmidt HA, Chernomor O, Schrempf D, Woodhams MD, Von Haeseler A, Lanfear R. 2020.** IQ-TREE 2: new models and efficient methods for phylogenetic inference in the genomic era. *Molecular Biology and Evolution* **37**:1530–1534 DOI [10.1093/molbev/msaa015](https://doi.org/10.1093/molbev/msaa015).
- Nikolaev SI, Mylnikov AP, Berney C, Fahrni J, Pawlowski J, Aleshin VV, Petrov NB. 2004.** Molecular phylogenetic analysis places *Percolomonas cosmopolitus* within Heterolobosea: evolutionary implications. *Journal of Eukaryotic Microbiology* **51**:575–581 DOI [10.1111/j.1550-7408.2004.tb00294.x](https://doi.org/10.1111/j.1550-7408.2004.tb00294.x).
- Park SJ, Park BJ, Pham VH, Yoon DN, Kim SK, Rhee SK. 2008.** Microeukaryotic diversity in marine environments, an analysis of surface layer sediments from the East Sea. *Journal of Microbiology* **46**(3):244–249 DOI [10.1007/s12275-007-0237-x](https://doi.org/10.1007/s12275-007-0237-x).

- Paskerova GG, Frolova EV, Kováčiková M, Panfilkina TS, Mesentsev ES, Smirnov AV, Nassonova ES. 2016. *Metchnikovella dogieli* sp. n. (Microsporidia: Metchnikovellida), a parasite of archigregarines *Selenidium* sp. from polychaetes *Pygospio elegans*. *Protistology* 10:148–157 DOI 10.21685/1680-0826-2016-10-4-4.
- Paskerova GG, Miroljubova TS, Diakin A, Kováčiková M, Valigurová A, Guillou L, Aleoshin VV, Simdyanov TG. 2018. Fine structure and molecular phylogenetic position of two marine gregarines, *Selenidium pygospionis* sp. n. and *S. pherusa* sp. n. with notes on the phylogeny of Archigregarinida (Apicomplexa). *Protist* 169:826–852 DOI 10.1016/j.protis.2018.06.004.
- Pawlowski J, Bolivar I, Fahrni JF, Cavalier-Smith T, Gouy M. 1996. Early origin of foraminifera suggested by SSU rRNA gene sequences. *Molecular Biology and Evolution* 13:445–450 DOI 10.1093/oxfordjournals.molbev.a025605.
- Penn O, Privman E, Ashkenazy H, Landan G, Graur D, Pupko T. 2010. GUIDANCE: a web server for assessing alignment confidence scores. *Nucleic Acids Research* 38:W23–W28 DOI 10.1093/nar/gkq443.
- R Core Team. 2021. R: a language and environment for statistical computing. Vienna, Austria: R Foundation for Statistical Computing. Available at <https://www.R-project.org/>.
- Reichenow E. 1929. Sporozoa. In: Doflein F, Reichenow R, eds. *Lehrbuch der Protozoenkunde: eine Darstellung der Naturgeschichte der Protozoen mit besonderer Berücksichtigung der parasitischen und pathogenen Formen. Part II.* Jena: Fünfte Auflage, 863–1153.
- Reichenow E. 1932. Sporozoa. In: Grimpe G, Wagler E, eds. *Die Tierwelt der Nord und Ostsee. m. b. H, Lief 21 (Teil II).* Leipzig: Akademische Verlagsgesellschaft, 188.
- Ronquist F, Teslenko M, Van der Mark P, Ayres DL, Darling A, Höhna S, Larget B, Liu L, Suchard MA, Huelsenbeck JP. 2012. MrBayes 3.2: efficient Bayesian phylogenetic inference and model choice across a large model space. *Systematic Biology* 61(3):539–342 DOI 10.1093/sysbio/sys029.
- Rotari YM, Paskerova GG, Sokolova YY. 2015. Diversity of metchnikovellids (Metchnikovellidae, Rudimicrosporea), hyperparasites of bristle worms (Annelida, Polychaeta) from the White Sea. *Protistology* 9:50–59.
- Rueckert S, Glasinovich N, Diez ME, Cremonte F, Vázquez N. 2018. Morphology and molecular systematic of marine gregarines (Apicomplexa) from southwestern Atlantic spionid polychaetes. *Journal of Invertebrate Pathology* 159:49–60 DOI 10.1016/j.jip.2018.10.010.
- Rueckert S, Leander BS. 2010. Description of *Trichotokara nothriae* n. gen. et sp. (Apicomplexa, Lecudinidae) –an intestinal gregarine of *Nothria conchylega* (Polychaeta, Onuphidae). *Journal of Invertebrate Pathology* 104:172–179 DOI 10.1016/j.jip.2010.03.005.
- Rueckert S, Simdyanov TG, Aleoshin VV, Leander BS. 2011. Identification of a divergent environmental DNA sequence clade using the phylogeny of gregarine parasites (Apicomplexa) from crustacean hosts. *PLOS ONE* 6:e18163 DOI 10.1371/journal.pone.0018163.

- Rueckert S, Wakeman KC, Leander BS. 2013.** Discovery of a diverse clade of gregarine Apicomplexans (Apicomplexa: Eugregarinorida) from Pacific eunicid and onuphid polychaetes, including descriptions of *Paralecudina* n. gen. *Trichotokara japonica* n. sp. and *T. eunicae* n. sp. *Journal of Eukaryotic Microbiology* **60**:121–136 DOI 10.1111/jeu.12015.
- Santos HF, Cury JC, Carmo FL, Rosado AS, Peixoto RS. 2010.** 18S rDNA sequences from microeukaryotes reveal oil indicators in mangrove sediment. *PLOS ONE* **5**(8):e12437 DOI 10.1371/journal.pone.0012437.
- Schrével J. 1969.** Biologie, cytologie, physiologie des Grégarines parasites d'Annélides polychètes. Faculté des Sciences de Lille. Lille, Université de Lille. Thèse doctorat. CNRS AO 2570.
- Schrével J, Vivier E. 1966.** Etude de l'ultrastructurale et du rôle de la région antérieure (mucron et épimérite) De Grégarines parasites d'Annélides Polychètes. *Protistologica* **2**(3):17–28.
- Sela I, Ashkenazy H, Katoh K, Pupko T. 2015.** GUIDANCE2: accurate detection of unreliable alignment regions accounting for the uncertainty of multiple parameters. *Nucleic Acids Research* **43**:W7–W14 DOI 10.1093/nar/gkv318.
- Simdyanov TG. 1995.** Two new species of gregarines with the aberrant structure of epicyte from the White Sea. *Parazitologiya* **29**:305–315.
- Simdyanov TG. 2007.** Class Gregarinae Dufour, 1828. In: *Protista: Handbook on zoology*. pt. 2. St. Petersburg: Nauka, 20–148 (in Russian with English summary).
- Simdyanov TG, Diakin AY, Aleoshin VV. 2015.** Ultrastructure and 28S rDNA phylogeny of two gregarines: *Cephaloidophora* cf. *communis* and *Heliospora* cf. *longissima* with remarks on gregarine morphology and phylogenetic analysis. *Acta Protozoologica* **54**:241–263 DOI 10.4467/16890027AP.15.020.3217.
- Simdyanov TG, Guillou L, Diakin AY, Mikhailov KV, Schréve J, Aleoshin VV. 2017.** A new view on the morphology and phylogeny of eugregarines suggested by the evidence from the gregarine *Ancora sagittata* (Leuckart, 1860) Labbé, 1899 (Apicomplexa: Eugregarinida). *PeerJ* **5**:e3354 DOI 10.7717/peerj.3354.
- Simdyanov TG, Paskerova GG, Valigurová A, Diakin A, Kováčiková M, Schrével J, Guillou L, Dobrovolskij AA, Aleoshin VV. 2018.** First ultrastructural and molecular phylogenetic evidence from the blastogregarines, an early branching lineage of pleisiomorphic Apicomplexa. *Protist* **169**(5):697–726 DOI 10.1016/j.protis.2018.04.006.
- Sokolova YY, Paskerova GG, Rotari YM, Nassonova ES, Smirnov AV. 2013.** Fine structure of *Metchnikovella incurvata* Caullery and Mesnil 1914 (microsporidia), a hyperparasite of gregarines *Polyrhabdina* sp. from the polychaete *Pygospio elegans*. *Parasitology* **140**:855–867 DOI 10.1017/S0031182013000036.
- Sokolova YY, Paskerova GG, Rotari YM, Nassonova ES, Smirnov AV. 2014.** Description of *Metchnikovella spiralis* sp. n. (Microsporidia: Metchnikovellidae), with notes on the ultrastructure of metchnikovellids. *Parasitology* **141**:1108–1122 DOI 10.1017/S0031182014000420.

- Stoeck T, Kasper J, Bunge J, Leslin C, Ilyin V, Epstein S. 2007.** Protistan diversity in the Arctic: a case of paleoclimate shaping modern biodiversity? *PLOS ONE* **2**:e728 DOI [10.1371/journal.pone.0000728](https://doi.org/10.1371/journal.pone.0000728).
- Stoeck T, Taylor GT, Epstein SS. 2003.** Novel eukaryotes from the permanently anoxic Cariaco Basin (Caribbean Sea). *Applied and Environmental Microbiology* **69**:5656–5663 DOI [10.1128/AEM.69.9.5656-5663.2003](https://doi.org/10.1128/AEM.69.9.5656-5663.2003).
- Tabei Y, Kiryu H, Kin T, Asai K. 2008.** A fast structural multiple alignment method for long RNA sequences. *BMC Bioinformatics* **9**(33):1–17 DOI [10.1186/1471-2105-9-33](https://doi.org/10.1186/1471-2105-9-33).
- Takishita K, Yubuki N, Kakizoe N, Inagaki Y, Maruyama T. 2007.** Diversity of microbial eukaryotes in sediment at a deep-sea methane cold seep: surveys of ribosomal DNA libraries from raw sediment samples and two enrichment cultures. *Extremophiles* **11**:563–576 DOI [10.1007/s00792-007-0068-z](https://doi.org/10.1007/s00792-007-0068-z).
- Von Kölliker A. 1845.** Die Lehre von der thierischen Zelle und den einfacheren thierischen Formelementen, nach den neuesten Fortschritten dargestellt. *Zeitschrift Für Wissenschaftliche Botanik* **1**(2):46–102.
- Von Kölliker A. 1848.** Beiträge zur Kenntniss niederer Thiere. *Zeitschrift für Wissenschaftliche Zoologie* **1**:1–37.
- Wakeman KC. 2020.** Molecular phylogeny of marine gregarines (Apicomplexa) from the Sea of Japan and the Northwest Pacific including the description of three novel species of *Selenidium* and *Trollidium akkeshiense* n. gen. n. sp. *Protist* **171**:125710 DOI [10.1016/j.protis.2019.125710](https://doi.org/10.1016/j.protis.2019.125710).
- Wakeman KC, Leander BS. 2013.** Identity of environmental DNA sequences using descriptions of four novel marine gregarine parasites, *Polyplacarium* n. gen. (Apicomplexa), from capitellid polychaetes. *Marine Biodiversity* **43**(2):133–147 DOI [10.1007/s12526-012-0140-5](https://doi.org/10.1007/s12526-012-0140-5).
- Wakeman KC, Yabuki A, Fujikura K, Tomikawa K, Horiguchi T. 2017.** Molecular phylogeny and surface morphology of *Thiriotia hyperdolphinae* n. sp. and *Cephaloidophora oradareae* n. sp. (Gregarinasina, Apicomplexa) isolated from a deep sea *Oradarea* sp. (Amphipoda) in the West Pacific. *Journal of Eukaryotic Microbiology* **65**(3):372–381 DOI [10.1111/jeu.12480](https://doi.org/10.1111/jeu.12480).
- Wickham H. 2016.** *ggplot2: elegant graphics for data analysis*. Cham: Springer International Publishing DOI [10.1007/978-3-319-24277-4](https://doi.org/10.1007/978-3-319-24277-4).
- Wray CG, Langer MR, De Salle R, Lee JJ, Lipps JH. 1995.** Origin of the foraminifera. *Proceedings of the National Academy of Sciences of the United States of America* **92**(7):141–145 DOI [10.1073/pnas.92.1.141](https://doi.org/10.1073/pnas.92.1.141).
- Wuyts J, Van de Peer Y, De Wachter R. 2001.** Distribution of substitution rates and location of insertion sites in the tertiary structure of ribosomal RNA. *Nucleic Acids Research* **29**:5017–5028 DOI [10.1093/nar/29.24.5017](https://doi.org/10.1093/nar/29.24.5017).
- Zuker M. 2003.** Mfold web server for nucleic acid folding and hybridization prediction. *Nucleic Acids Research* **31**(13):3406–3415 DOI [10.1093/nar/gkg595](https://doi.org/10.1093/nar/gkg595).